

**THE EFFECT OF BIOLOGICAL SEX ON  
INFLUENZA B VIRUS  
PATHOGENESIS IN MICE**

**by**

**Aihui Wang**

**A thesis submitted to Johns Hopkins University in conformity with the  
requirements for the degree of Master of Science**

**Baltimore, Maryland**

**April 2021**

© 2021 Aihui Wang  
All rights reserved

## ABSTRACT

**Background:** Biological sex can impact the pathogenesis and outcome of viral infection by modulating immune responses that control inflammation, antibody production, and tissue repair. Influenza B viruses (IBVs) are classified into B/Yamagata and B/Victoria lineages, which co-circulate during the influenza season with varying dominance. Epidemiological data show greater circulation and diseases caused by IBV in recent years, with higher hospitalization and mortality rate in males than females, especially in children and the elderly. Compared with influenza A viruses (IAVs), however, studies of IBV are still lacking.

**Methods:** We developed a mouse model to study the sex differences in the pathogenesis of IBV infection. Adult male and female C57BL/6 mice were intranasally infected with  $10^5$  TCID<sub>50</sub> units of the B/Brisbane/60/2008 (Victoria lineage), carrying the PB2 F406Y mutation that increases virulence in mice. Morbidity and mortality were monitored for 15 days. Lungs were harvested and homogenized at 1, 3, 5, and 7 days post infection (dpi) to characterize viral kinetics. Lungs, spleens and sera were collected at 3 and 7 dpi for cytokine quantification to analyze the innate immune response. Neutralizing antibody titers were also determined in sera collected at 21 dpi.

**Results:** Male mice experienced greater morbidity, i.e., had greater body mass loss and hypothermia, than females. Biological sex affected lung viral kinetics, in which males consistently had higher virus titers than females. Males showed aberrant innate responses in the lungs, with lower local induction of cytokines than females in the lungs at 3 dpi, but sustained inflammation at 7 dpi of IBV infection. Both males and females showed peripheral induction of cytokines in the spleen and sera at 3 dpi and to a stronger extent at 7dpi, with no sex differences observed. Neutralizing antibody titers were significantly lower in males than females at 21 dpi.

**Conclusion:** Taken together, these data suggest that males experience more severe disease than females following IBV infection. Impaired viral clearance combined with compromised innate and adaptive immune responses in males compared with females may contribute to worse IBV outcomes. The effects of biological sex on IBV pathogenesis and responses to vaccines should be explored in humans.

**Primary Reader: Dr. Sabra L. Klein**

**Secondary Reader: Dr. Fengyi Wan**

## ACKNOWLEDGEMENT

I would like to express my deepest gratitude to my advisor, Dr. Sabra Klein, for her continuous mentorship and support during my graduate research. Thank you for providing me with abundant academic opportunities, as well as the professional guidance. I would like to thank Yishak Woldetsadik, for doing previous work, mentoring me patiently, and teaching me the techniques detailly. I would like to thank Rebecca Ursin, for keeping concerned with this project, sharing her thoughts, and providing help when I got into trouble. Thank you to my lab mates, Patrick Creisher, Santosh Dhakal, Han-Sol Park, Abhinaya Ganesan, Morgan Sherer, Henning Jacobsen, Christopher Caputo, and Janna Shapiro, for their encouragement, insights, and all the help. Thank you to Dr. Andrew Pekosz, Dr. Kim Davis and their lab members, for their inspirations during the joint lab meetings. I would also like to thank my secondary reader, Dr. Fengyi Wan, for his input and advice.

I thank my friends here and away, Xuetong, Haoran, Zhihao, Amy, Yuyan, and Elaine, for their listening, understanding, and the encouragement. Thank you to Yan, for your accompany during my hardest moment. Last but not least, I would like to thank my parents, for being my solid backing and my best friends, and always supporting me to pursue my goals.



## TABLE OF CONTENTS

<b>S. No.</b>	<b>Title</b>	<b>Page No.</b>
1	Preface	ii-iv
2	List of Tables	vi
3	List of Figures	vii
4	Abbreviations	viii-ix
5	Introduction	1-15
6	Methods	16-19
7	Results	20-29
8	Discussion	30-34
9	Figure and Table Legends	35-38
10	Bibliography	39-49
11	Supplemental Tables	50-58
12	Curriculum Vitae	59-61

## LIST OF TABLES

<b>S. No.</b>	<b>Table/Figure</b>	<b>Title</b>	<b>Page No.</b>
1	Table 1	Structural and functional differences in influenza A (IAV), B (IBV), C (ICV), and D (IDV) viruses.	13
2	Table 2	Comparison of Victoria and Yamagata lineage influenza B viruses.	14
3	Table 3	Comparison of the process for IAV transcription and replication.	14
4	Table 4	Featured cytokines in influenza infection.	15
5	Table 5	The effect of sex associated factors on influenza pathogenesis.	34
6	Sup. Table 1	Raw cytokine concentrations in spleens.	50-52
7	Sup. Table 2	Raw cytokine concentrations in sera.	53-55
8	Sup. Table 3	Raw cytokine concentrations in lungs.	56-58

## LIST OF FIGURES

1	Figure 1	Experimental designs.	23
2	Figure 2	Morbidity and lung virus titers of B/Brisbane infected adult male and female C57BL/6 mice.	24
3	Figure 3	Cytokine fold change profile in spleens.	25
4	Figure 4	Cytokine fold change profile in sera.	26
5	Figure 5	Cytokine fold change profile in lungs.	27
6	Figure 6	Sex difference in the induction of pulmonary cytokines after B/Brisbane infection.	28
7	Figure 7	Neutralizing antibody titers in the sera at 21 dpi.	29

## ABBREVIATIONS

ADCC	Antibody-dependent Cell-mediated Cytotoxicity
ASC	Apoptosis-associated Speck-like Protein Containing a CARD
BAFF	B-cell Activating Factor
CDC	Centers of Disease Control and Prevention
CPE	Cytopathic Effects
cRNA	Complementary RNA
CTL	Cytotoxic T Cells
DC	Dendritic Cell
DMEM	Dulbecco's Modified Eagles Medium
dpi	Days Post Infection
ePol II	Eukaryotic Polymerase II
Gal	Galactose
G-CSF	Granulocyte Colony-Stimulating Factor
GM-CSF	Granulocyte-Macrophage Colony-Stimulating Factor
HA	Hemagglutinin
HEF	Hemagglutinin-Esterase-Fusion
IAV	Influenza A Virus
IBV	Influenza B Virus
ICV	Influenza C Virus
IDV	Influenza D Virus
IFN	Interferon
IgG/A	Immunoglobulin G/A
IL	Interleukin
IRF7	IFN-Regulatory Factor 7
M1	Matrix Protein1
M2	Matrix Protein 2
MAVS	Mitochondrial Antiviral-Signaling

M-CSF	Macrophage Colony-Stimulating Factor
MDCK	Madin-Darby Canine Kidney
MFR	Male to Female Ratio
MOI	Multiplicity of Infection
NA	Neuraminidase
NEP	Nuclear Export Protein
NF- $\kappa$ B	Nuclear Factor- $\kappa$ B
NK	Natural Killer
NLRP	Nucleotide-binding Oligomerization Domain, Leucine Rich Repeat and Pyrin Domain Containing Protein
NP	Nucleocapsid Protein
NS	Non-structural Protein
PA	Polymerase A
PAMP	Pathogen-Associated Molecular Pattern
PB1	Polymerase B1
PB2	Polymerase B2
PRR	Pattern-Recognition Receptor
RANKL	Receptor Activator of Nuclear Factor Kappa-B Ligand
RIG-I	Retinoic acid-Inducible Gene I
RNP	Ribonucleoprotein
ssRNA	Single-stranded Ribonucleic Acid
TCID <sub>50</sub>	Tissue Culture Infectious Dose 50
TLR	Toll-Like Receptor
TNF	Tumor Necrosis Factor
VEGF	Vascular Endothelial Growth Factor
vPol	Viral Polymerase
vRNP	Viral Ribonucleoproteins
WHO	World Health Organization

# INTRODUCTION

## Overview of Influenza Viruses

Influenza viruses, including influenza A, B, C and D viruses, are in the *Orthomyxoviridae* family (**Table 1**). Respectively, they are the only species in Alphainfluenzavirus, Betainfluenzavirus, Gammainfluenzavirus and Deltainfluenzavirus genera. Influenza A Virus (IAV) has a variety of hosts, including avian, swine, and human. In contrast, humans are the only known host of Influenza B Virus (IBV). It has been reported sporadically that IBV can infect seals, but there is still no evidence of the transmission from seals to humans [1-4]. Despite the limited host range, IBV can cause severe disease that is comparable to IAV, which makes IBV a public health concern. Influenza C Virus (ICV) was first isolated from human throat washings in 1947 and classified as a new type of influenza by Francis *et al* in 1950 [5-7]. Serological studies showed that the antibodies to ICV were prevalent in adults, indicating possible childhood ICV infections [5, 8-10]. However, compared to IAV and IBV, ICV only induces mild symptoms, and is not a significant pathogen of seasonal influenza. Influenza D Virus (IDV) is a recently identified influenza virus, which mainly infects swine and cattle. In 2013, when IDV was first discovered, it was recognized as a novel strain of ICV [11]. Subsequently, IDV was characterized as a new species in the *Orthomyxoviridae* family in 2014[12]. To date, there are no reports of human-related IDV infection.

Influenza viruses are enveloped viruses with segmented, single stranded, negative sense RNA genome, which code for different functional proteins. Single-stranded RNAs (ssRNAs) are covered by Nucleocapsid Proteins (NP). The viral polymerase (P) subunits, PA, PB1 and PB2, are attached to the ribonucleoprotein (RNP) and essential for virus replication. IAV and IBV have 8 segments in the genome, while ICV and IDV have 7 segments (**Table 1**). These segments

are enveloped by the matrix protein (M1) covered with a lipid bilayer from the infected host cell, with glycoproteins protruding on the surface. The virions of IAV and IBV are indistinguishable under electron microscope, which are usually in spherical or filament shapes and have two types of glycoproteins, including hemagglutinin (HA) and neuraminidase (NA), on the surface, which are the major surface antigens of influenza virus. In IAV, M2 proteins lay on the matrix, whereas in IBV BM2 and NB proteins are the matrix proteins. Distinct from IAV and IBV, the virions of ICV and IDV are more pleomorphic. Filamentous structures are more common in ICV and IDV and they can form long cordlike structures on the surface of infected cells. Beyond that, the surface glycoproteins on ICV and IDV are organized in a hexagonal pattern and are only consist of hemagglutinin-esterase-fusion (HEF) proteins. Similar to IAV, there are CM2 proteins overlaying the matrix (**Table 1**).

The influenza viruses can be further divided according to the genetic and antigenic differences. In IAV, 18 subtypes of HA (H1 to H18) and 11 subtypes of NA (N1 to N11) have been identified. And IAVs are divided into a variety of subtypes based on their HA and NA subtypes, for example, H1N1 and H7N9. In contrast, IBVs are only divided into two lineages, namely Yamagata and Victoria, by the sequence and antigenicity of HA [13]. ICV and IDV, which have HEF, instead of HA and NA, as the surface antigenic proteins, are further typed into lineages according to HEF. At present, there are six known lineages of ICV and four known lineages of IDV [14, 15].

The genomes of all influenza viruses are segmented ssRNAs. RNA virus polymerase lacks the activity of proofreading, resulting in an error-prone replication[16]. Therefore, HA proteins are of great variance with a high mutation rate. Under the immune pressure from the host immune response, these mutations can be selected and accumulated, leading to minor

changes on the antigen, termed antigenic drift. The variance of antigen can also be developed by reassortment, termed antigenic shift, which takes advantage of the segmented genome. When two different strains of influenza virus infect a same cell simultaneously, their genome segments can mix up and form a new strain with distinct characteristics. Antigenic shift frequently occurs in IAV, because IAV has been adapted to aquatic avian, which serves as a gene pool for IAV evolution. Antigenic shift of IAV usually induces influenza outbreaks. IBV also undergoes antigenic drifts and antigenic shifts. Evidence shows that antigenic shifts are of more importance in the evolution of IBV[17, 18]. However, the evolution rate is much slower than IAV because with limited animal reservoir, IBV lacks non-human gene pool [18, 19]. Within a type of influenza, the reassortment can occur within a lineage or between lineages[20]. Intertypical reassortment between influenza viruses has not been reported, which can be attributed to the incompatible packaging signals in different types of influenza virus [21].

Only IAV and IBV induce severe diseases in humans and are of epidemiologic interest. Historically, there have been four influenza pandemics: 1918 H1N1, 1957 H2N2, 1968 H3N2, and 2009 H1N1; all were caused by IAV substrains [22]. The pandemic is partially attributed to the fast evolution rate of IAV. The antigenic shifts lead to significant change in the surface antigens (HA and/or NA). Because humans are immunologically naïve to the new antigen, the novel IAV strain can readily infect and replicate in the host cells, often with greater transmissibility and virulence than seasonal strains, contributing to defining these as pandemic strains. The pandemic IAV strain will continue to circulate worldwide, undergoing antigenic drift, and eventually becoming a seasonal strain of IAV [23, 24]. IBV, which has limited hosts and thereby lower evolution rate, is not known to cause pandemics, while it co-circulates with IAV to cause seasonal influenza and can induce severe disease, similar to IAV. The receptors of



the two lineages of IBV are different (**Table 2**). Victoria lineage viruses recognize the Sialyl  $\alpha$ -2,3 Galactose as well as the Sialyl  $\alpha$ -2,6 Galactose, while Yamagata lineage viruses only recognize the Sialyl  $\alpha$ -2,6 Galactose. The difference in receptor binding may partially explain the epidemiological differences present between the two lineages. Generally, younger people are more susceptible to Victoria lineage viruses, with peak cases in individuals below 10 years of age. In contrast, the age distribution of disease caused by Yamagata lineage viruses peak among individuals younger than 10 years of age and again among middle-aged adults [25, 26]. Victoria lineage induces more severe disease and greater hospitalization rates than Yamagata lineage viruses [27]. Compared with Yamagata lineage viruses, the transmission of Victoria lineage viruses is more sustained within a region [26]. The circulating IAVs and IBVs, influenza-associated hospitalizations and mortalities are under continuous surveillance by the Centers of Disease Control and Prevention (CDC) in the United States as well as in other countries. Seasonal influenza is a substantial health burden in humans. As is estimated by World Health Organization (WHO), each year globally, seasonal influenza results in 3-5 millions of severe cases and 290 000-650 000 deaths due to respiratory diseases[28]. Aside from IAV, which is drawing a lot of attention, IBV is causing greater circulation and diseases in recent years[25, 29]. In 2019-20 season, 61.7% of pediatric mortality was caused by IBV[30]. Therefore, it is of great value and indispensable to have comprehensive understanding of IAV and IBV to control the influenza transmission and infection more efficiently.

### **The Life Cycle of Influenza A Viruses**

After invading into host organism, the HA of IAVs bind to the sialyl-galactose residues on the surface of host cells, primarily respiratory epithelial cells. Sialic acid linked to either the 3' carbon or 6' carbon of the galactose can be recognized by influenza HA, namely Sialyl  $\alpha$ -2,3

Gal and Sialyl  $\alpha$ -2,6 Gal. Sialyl  $\alpha$ -2,3 Gal is regarded as the avian receptor and Sialyl  $\alpha$ -2,6 Gal is regarded as the human receptor of influenza viruses, as avian influenza viruses preferentially bind the Sialyl  $\alpha$ -2,3 Gal and human influenza viruses preferentially bind the Sialyl  $\alpha$ -2,6 Gal [31, 32]. Sialyl  $\alpha$ -2,3 Gal is found in the avian intestinal epithelial cells, where avian influenza viruses replicate in their reservoir hosts [33, 34]. The two types of sialic acids, however, are present in human airways. Epithelial cells in the upper respiratory tract, including the trachea and bronchi, mainly express Sialyl  $\alpha$ -2,6 Gal, while Sialyl  $\alpha$ -2,3 Gal is enriched in the lower respiratory track, primarily in alveolar cells [35]. The different distribution of sialic acid receptors contributes to the host specificity of influenza viruses. Both the avian Sialyl  $\alpha$ -2,3 Gal and the human Sialyl  $\alpha$ -2,6 Gal present in the swine trachea [34], which is why swine serve as a mixing vessel for the reassortment of avian influenza virus and human influenza virus. New variants of IAVs, including the 2009 H1N1 pandemic strain are derived from swine. When avian IAVs develop the ability to bind the Sialyl  $\alpha$ -2,6 Gal by reassortment, these viruses can infect humans and cause serious epidemic and even pandemic levels of transmission.

After the binding of influenza HA to the Sialyl-galactose residue, the virus is engulfed in an endosome and a series of structural and chemical changes are initiated. First, host protease cleaves the HA at R329 and 1G into a fusion-competent form [36]. Virus acidification, driven by M2 ion channels, provides a low pH environment, which allows the HA to expose the fusogenic peptide [36, 37]. Fusogenic HA mediates the fusion of viral capsid and the endosomal membrane. The viral ribonucleoproteins (vRNPs) enter the host cell cytoplasm through the fusion pore, where the vRNP usurps the nuclear import machinery of the host cell to enter the nucleus [38].

The single-stranded negative-sense RNA segments of the influenza genome are the templates both for the viral mRNA transcription and for the synthesis of complementary RNA (cRNA), which serves as the replication template to produce multiple vRNAs. The biochemical process of transcription and replication are distinct (**Table 3**). Transcription occurs prior to replication, which is initiated by the binding of viral polymerase (vPol) to the host eukaryotic polymerase II (ePol II) and is primed by the capped host pre-mRNA segments [39]. The host pre-mRNA primer is caught by PB2 and then cleaved by PA[40]. Viral mRNA is synthesized by PB1 using vRNA as the template, which then seizes the host ribosomes to express viral proteins. Replication is a two-step process and is primer-independent [40]: 1) cRNA is synthesized by PB1 and 2) new vRNA synthesis uses cRNA as the template. The rate of replication is much slower than the transcription [41].

After vRNA synthesis, PB1, PB2, PA, and NP binds to the vRNA to form the vRNP in the host nucleus. Similar to the import, the vRNP exploits the host nucleus export protein, namely exportin-1, to migrate into the host cytoplasm [38]. Surface proteins, including NA, HA, and M2, are inserted into the plasma membrane. The virion is assembled at the plasma membrane and nucleated driven by M1 proteins. Finally, NA cleaves the sialic acid from the glycoproteins, releasing the budding virus from the host cell.

### **The Innate immune responses to IAV infection**

The innate immune responses that recognize and respond to IAVs are critical for antiviral immunity. Pathogen-associated molecular patterns (PAMPs) are recognized by pattern-recognition receptors (PRRs), including surface PRRs, such as Toll-like receptors (TLRs) and cytosolic PRRs [42, 43]. For IAVs, TLR3 and TLR7 are the major functional surface PRRs. TLR3 recognizes dsRNA in the endosome of IAV infected cells, providing signals to restrict

viral replication and prime the adjacent cells, and expressing chemokines to recruit innate and adaptive immune cells[44-46]. TLR7 recognizes the ssRNA genomes contained in IAV virions, activates nuclear factor- $\kappa$ B (NF- $\kappa$ B) and IFN-regulatory factor 7 (IRF7) via MyD88 signaling to express type I interferons (IFNs), pro-inflammatory cytokines, and multifunctional interleukin 12 (IL-12). Type I IFNs can directly interfere the viral replication, prime the adjacent cells, and enhance the cell-mediated immunity[47, 48]. Pro-inflammatory cytokines, including tumor necrosis factor (TNF) and IL-6, improve the immune cell function, but also result in the systemic symptoms of influenza[49]. IL-12 is the key factor to induce the T<sub>H</sub>1 responses[50]. It also promotes natural killer (NK) cells and T cells to release type II IFN (IFN $\gamma$ ), which serves as a non-specific activator for many immune cells [50] (**Table 4**). TLR7 also plays an important role in antibody production [51, 52]. TLR7 deficiency leads to compromised early-B-cell response and lower level of HA-specific antibody production [53]. Administration of TLR7 agonists facilitate more robust immune responses to IAV infection in mice [54].

Other PRRs, including retinoic acid-inducible gene I (RIG-I) and Nucleotide-binding oligomerization domain, Leucine rich Repeat and Pyrin domain containing Proteins (NLRPs) have roles in cytosolic PAMP recognition. RIG-I recognizes the replicated viral ssRNA bearing 5'-triphosphate[55-57], activating NF- $\kappa$ B and IRF3 via mitochondrial antiviral-signaling (MAVS) [58]. IAV infection also stimulates the NLRP3 oligomerization. Oligomerized NLRP3 recruits apoptosis-associated speck-like protein containing a CARD (ASC) and Caspase 1 to form an NLRP3 inflammasome, leading to caspase-1 activation and pro-inflammatory IL-1 $\beta$  and IL-18 secretion [59, 60]. Evidence also shows that ASC and Caspase 1 are indispensable in developing the adaptive immune responses against IAV infection[61].

Innate immune system reacts rapidly after the exposure to IAV and leads to early signs of influenza infection, including feverishness, fatigue, headaches, and myalgias, which are induced by pro-inflammatory cytokines [62]. During influenza infection, cytokines help with the antiviral process either by interfering viral replication or by enhancing the cell-mediated and/or humoral immune responses (**Table 4**). However, the rapid and excess production of cytokines leads to cytokine storm, which is the pathogenic sin for acute respiratory syndrome, tissue damages, and organ dysfunctions. Pro-inflammatory cytokines stand in the eye of the storm. TNF plays a key role in the cytokine storm, contributing to the morbidity of IAV infection by inducing hyperactive inflammation, tissue damage, and lung consolidation[63-65]. IFNs activate the IFN-induced gene expression, which is indispensable for IAV clearance, nevertheless, excessive IFN signaling causes uncontrolled inflammation and irreversible lung tissue damage[66-69]. IL-1 and IL-18, which are the downstream products of NLRP3 inflammasome, are also responsible for the acute pulmonary immunopathology[70, 71]. However, IL-6 serves as a protective factor in the hyperinflammation by producing neutrophil survival and reducing the lung pathology[72, 73]. In addition, excessive chemokines can recruit superfluous immune cells to the site of infection, which exacerbates the detrimental inflammation[74].

During IAV infection, the non-specific innate immunity is first initiated via PAMP-PRR recognition, priming the uninfected cells and inducing the specific and more efficient adaptive immunity. Innate immune responses play an important role in the early stage of infection to interfere viral replication and assist with viral clearance. However, the inflammation induced by innate immune responses contributes to immunopathology, and even can result in the mortality of influenza.

### **The Adaptive Immune Responses to IAV Infection**

The adaptive immune response typically takes 5-7 days to develop, providing a highly specific and efficient effect to restrict viral replication, clear the viruses, and develop memory to protect from re-infection. The humoral response is predominated by HA-specific antibody and NA-specific antibody. Anti-HA antibodies typically bind to the head domain of HA, which contains the receptor-binding site and is variable between IAV strains[75, 76]. These antibodies neutralize the viral infection either by blocking the IAV entry to the cell or by inducing the Fc receptor-mediated phagocytosis[77]. Some HA specific antibodies that bind to the HA stem domain, which is the conserved region, also have the protective effect via neutralizing viruses and inducing antibody-dependent cell-mediated cytotoxicity (ADCC) [78-80]. HA stem-binding antibodies are the major components of cross-reactive antibodies against influenza, and they have a broad-spectrum protection across IAV strains and even across both IAV and IBV [81-85]. Anti-NA antibodies also have protection against influenza infection by inhibiting the enzymatic activity. NA active site-binding antibodies that broadly neutralize multiple different IAV and IBV strains [86, 87]. Influenza infection also induces antibodies against NP, matrix proteins, and other virion components [75, 88-90]. Antibody responses are mount within 1-2 weeks after influenza infection. IgG is the dominant subtype of protective influenza-specific antibodies in lungs and serum, while IgA plays a more important role in mucosal protection at the entrance of infection, i.e., the respiratory tract [91, 92]. The antibody protection induced by natural infection of influenza can last for decades [75].

The clearance of infected cells requires a cellular response, mediated by CD4<sup>+</sup> T cells and CD8<sup>+</sup> T cells. Dendritic cells process and present the exogenous and endogenous influenza virus antigens in the class I and class II major histocompatibility complex (MHC) molecules to CD8<sup>+</sup> and CD4<sup>+</sup> T cells, respectively. CD4<sup>+</sup> T cells recognize the influenza epitope in the

context of class II MHC, further differentiating to Th1 cells to protect against viral infection [93]. Th1 cells produce IFN- $\gamma$  which has the antiviral activity and can activate macrophages [94, 95]. IAV-activated CD4<sup>+</sup> T cells also produce IL-2 to stimulate CD8<sup>+</sup> T cell proliferation and differentiation [96]. Activated and armed CD8<sup>+</sup> T cells, also called cytotoxic T cells (CTLs), recognize the influenza peptide presented in class I MHC. CTLs can either directly kill the infected cell via cytolysis using preformed perforin and granzymes or induce apoptosis via Fas/FasL interaction[97]. Evidence shows that CTLs are more cross-reactive to different influenza strains compared to the antibodies[98]. However, the memory pool of CTLs that recognize IAVs contract within a few years, and the longevity of T cell memory after influenza infection is still unclear [99, 100]. Besides, dysregulated CTL can also accelerate the pulmonary immunopathology via its cytotoxic activity or pro-inflammatory cytokine secretion[101, 102].

Adaptive immunity is not initiated immediately after infection, but it is the most powerful defense. Neutralizing antibodies, which are highly specific to a certain IAV epitope, interfere the viral life cycle to slow down the spread of virions. CD4<sup>+</sup> T cells predominantly differentiate to Th1 cells during IAV infection, providing sufficient IFN- $\gamma$  to impede viral replication. Meanwhile, CD8<sup>+</sup> T cells are activated and armed to specifically clear the IAV infected cells by direct contact and the cytotoxicity. In addition, adaptive immunity can develop long-term memories to prepare for the next exposure to the identical pathogen. However, the adaptive immune responses need to be well-regulated to avoid the drastic tissue damage.

### **Animal Models to Study Influenza Pathogenesis**

The pathogenesis of IAV infection has been characterized in various mammalian animal models, including mice, rats, guinea pigs, ferrets, hamsters, and rhesus macaques [103]. Mice are the most commonly used model, and inbred mouse strains, including BALB/C, C57BL/6, and

DBA/2, are frequently used to study IAV pathogenesis via intranasal infection. DBA/2J mice are more susceptible to IAV infection compared to BALB/C and C57BL/6 mice [104, 105].

However, animal models for IBV pathogenesis are lacking because of the limited host range of IBV. Mice and ferrets have been used for IBV pathogenic models[106-108]. IBV must be adapted by serial passaging or inducing mutation to increase the infectivity in non-host animals[106-108].

### **Sex Difference in the Response to Influenza Infection**

Epidemiological evidence shows age-stratified sex differences in the morbidity and mortality of IAV infection both in pandemics and seasonal epidemics [109-113]. In children, the confirmed cases are significantly higher in boys than girls [111, 112]. While in adults, the male to female ratio (MFR) decreases and even reverses [111]. In the mouse models of IAV infection, females have greater morbidity and slower recovery than males [114-116]. This female bias in IAV disease pathogenesis is caused by sex steroid hormone-mediated greater inflammation and reduced activation of repair pathways [114-118]. For example, greater production of amphiregulin and testosterone production in males have been shown to independently protect male mice in H1N1 infection [114]. While amphiregulin promotes repair of damaged tissue caused by infection and immune-activation, testosterone dampens inflammation [117]. In female mice, infection with IAV disrupts their reproductive cycle and administration of estradiol, estriol, or progesterone can suppress the inflammatory response to protect them from severe pathogenesis [115, 118, 119]. Females produce more neutralizing antibodies, and the total antibody response against IAV is stronger in females than in males, which is also mediated by estradiol in female mice [116, 120]. While progesterone treatment reduces the adaptive immune



responses in female mice, compromising the protection from re-exposure[118]. And the cross protection of humoral immune response is greater in females compared to males [116].

In IBV, sex differences in disease pathogenesis are age dependent. Generally, males are less likely to be infected with IBV [121]. In children, however, boys have a higher frequency of IBV infections than girls [122]. The hospitalization rate also is higher in males than in females, except for among young adults, age 18-39, in which females experience greater disease than males [25, 112, 123]. Females also tend to have a lower mortality from IBV infection [124].

Comparing to IAV, there are fewer pathogenic studies of IBV infection due to the lack of suitable animal models. Recent study in female mice found that IBV infection induces severe diseases and decreases concentrations of progesterone and estradiol during pregnancy, suggesting that sex hormone can be disturbed by IBV infection [125]. Unpublished data from our collaborator Dr. Daniel Perez show greater morbidity in the male DBA/2J mice compared to the females infected with mouse-adapted B/Brisbane/60/2008 (Victoria lineage), which is different from IAV infection (see above).

Therefore, to better understand the effect of biological sex on IBV infection, we established a pathogenetic model in male and female C57BL/6 mice. We compared the morbidity, lung viral kinetics, cytokine responses, and antibody production between male and female mice. Results were also compared with the published corresponding data of IAV.

**Table 1.** Structural and functional differences in influenza A (IAV), B (IBV), C (ICV), and D (IDV) viruses.

	IAV	IBV	ICV	IDV
<b>Hemagglutinin</b>	HA	HA	HEF	HEF
<b>Neuraminidase</b>	NA	NA		
<b>Polymerase</b>	PB1, PB2, PA	PB1, PB2, PA	PB1, PB2, PA	PB1, PB2, PA
<b>Matrix protein</b>	M1	M1	M1	M1
<b>Ion channel</b>	M2	BM2, NB	CM2	CM2
<b>Genome</b>	ssRNA (-) 8 segments	ssRNA (-) 8 segments	ssRNA (-) 7 segments	ssRNA (-) 7 segments
<b>Nucleoprotein</b>	NP	NP	NP	NP
<b>Nuclear export protein</b>	NS2/NEP	NS2/NEP	NS2/NEP	NS2/NEP
<b>Non-structural protein</b>	NS1	NS1	NS1	NS1
<b>Hosts</b>	Avian, human, swine, horse, seals	Human, seals	Human	Bovine, swine
<b>Receptors</b>	Sialic acid, $\alpha$ -2,3 and/or $\alpha$ -2,6	Sialic acid (Victoria: $\alpha$ -2,3 and $\alpha$ -2,6; Yamagata: $\alpha$ -2,6)	9-O-acetyl- neuraminic acid	9-O-acetyl- neuraminic acid

**Table 2.** Comparison of Victoria and Yamagata lineage influenza B viruses.

	<b>Victoria</b>	<b>Yamagata</b>
<b>Receptor</b>	$\alpha$ -2,3 and $\alpha$ -2,6	$\alpha$ -2,6
<b>Age distribution</b>	Younger, positively skewed unimodal	Older, bimodal
<b>Hospitalization</b>	More severe	Less severe
<b>Transmission</b>	More regional	Broader

**Table 3.** Comparison of the process for IAV transcription and replication.

	<b>Transcription</b>	<b>Replication</b>
<b>Timing</b>	Prior	Posterior
<b>Process</b>	One-step: vRNA→mRNA	Two-step: vRNA→cRNA; cRNA→vRNA
<b>Primer dependence</b>	Host pre-mRNA primer	Primer-independent
<b>ePol II dependence</b>	vPol activated by ePol II	ePol II-independent
<b>Rate</b>	High	Low

**Table 4.** Featured cytokines in influenza infection.

<b>Cytokine</b>	<b>Major source</b>	<b>Major functions</b>	<b>Immuno-pathogenesis</b>	<b>Activation time</b>
<b>IL-1<math>\beta</math></b>	Macrophages	Pro-inflammatory cytokine Promote monocyte differentiation Promote B cell and T cell functions	Tissue damage	Immediate
<b>IL-6</b>	Macrophages	Pro-inflammatory cytokine Promote monocyte differentiation Promote B cell and T cell differentiation Protect hyperinflammation	Tissue damage	Immediate
<b>TNF</b>	Epithelial cells, macrophages, NK cells	Pro-inflammatory cytokine Induce the release of IL-1 and IL-6 Promote neutrophil and macrophage functions	Tissue damage Leading role in cytokine storm	Immediate
<b>IL-18</b>	Macrophages	Pro-inflammatory cytokine Upregulate IL-1 and TNF; downregulate type I IFN Enhance cell-mediated immunity	Tissue damage	Immediate
<b>IL-12</b>	Macrophages, Dendritic cells (DCs)	Enhance cell-mediated immunity	Tissue repair	Immediate
<b>IL-33</b>	Necrotic barrier cells, macrophages	Enhance T <sub>H</sub> 2 immune response Regulate excessive inflammatory response	Tissue repair	Early stage
<b>IL-4</b>	T <sub>H</sub> 2 CD4 T cells	Promote B cell differentiation Reduce cell-mediated immunity	Tissue repair	Late stage
<b>IL-10</b>	Treg, B cells, macrophages,	Anti-inflammatory cytokine	Upregulated in cytokine storm	Late stage
<b>Type I IFN</b>	Epithelial cells, DCs	Pro-inflammatory cytokine Antiviral cytokine Enhance cell-mediated immunity Upregulate chemotactic cytokines	Tissue damage	Immediate
<b>Type II IFN</b>	T <sub>H</sub> 1 CD4 T cells, NK cells	Antiviral cytokine Upregulate pro-inflammatory cytokines Promote DC activation Enhance cell-mediated and humoral immunity	Tissue damage	Early stage
<b>Type III IFN</b>	Epithelial cells, DCs	Antiviral cytokine	/	Immediate

## METHODS

### Animals

Adult (8-12 weeks) male and female C57BL/6 mice were purchased from Charles River Laboratories. All animals were housed at up to 5 mice per microisolator cage under standard biosafety level 2 housing conditions, with food and water provided *ad libitum*. All experiments were performed in compliance with the standards outlined in the National Research Council's Guide to the Care and Use of Laboratory Animals. All animal procedures were approved by the Johns Hopkins Animal Care and Use Committee (MO18H250). All efforts were made to minimize animal suffering.

### Virus

B/Brisbane/60/2008 with PB2 F406Y mutation (mt-B/Bris) virus was used in this study for infection and antibody titration. PB2 F406Y mutation was induced to B/Brisbane/60/2008 virus by Dr. Daniel Perez to enhance the pathogenesis in mice. The working stock was generated by infecting Madin-Darby Canine Kidney (MDCK) cells at a multiplicity of infection (MOI) of 0.01 and the infected cell supernatant was collected, centrifuged, and the virus containing supernatant was collected. The quantity of viruses is determined by units of tissue culture infectious dose (TCID<sub>50</sub>).

### Animal infection and processing

Mice were anesthetized with ketamine (80mg/kg)/ xylazine (13mg/kg) cocktail injected intraperitoneally and inoculated intranasally with 10<sup>4</sup> and 10<sup>5</sup> TCID<sub>50</sub> units of B/Brisbane/60/2008 in 30uL of the virus in Dulbecco's modified Eagles Medium (DMEM). For morbidity study, body mass and rectal temperature changes were daily recorded up to 14 days

post infection (dpi). For time course experiments, mice were randomly assigned to be euthanized at 1, 3, 5, and 7 dpi. Mice were anesthetized using ketamine–xylazine cocktail before retrobulbar bleeding. Blood was collected into heparinized tubes and was centrifuged to separated plasma. Plasma was stored at -80°C and used to measure cytokines. Left lung and spleen were collected, snap-frozen and stored at -80°C. Right lung lobes were inflated and fixed with zinc-buffered formalin (Z-fix, Anatech, MI, USA) under a constant pressure of 25 cmH<sub>2</sub>O for at least 24 hours. Plasma was also collected at 21 dpi to measure the antibodies.

### **Lung virus titration**

Left lungs were homogenized in 500ul of serum-free DMEM. Infectious viral particles in the supernatants were detected using TCID<sub>50</sub> assay. Lung samples were 10-fold serial-diluted and transferred into 96-well tissue-culture plates in six replicates to infect a confluent monolayer of MDCK cells. Plates were incubated at 32°C for 6 days, fixed with 4% formaldehyde, and stained with naphthol blue black. Units of TCID<sub>50</sub> were calculated based on the cytopathic effects (CPE) of influenza B virus.

### **Detection of cytokines and chemokines**

Left lungs and spleens were homogenized in 500ul of serum-free DMEM, followed by centrifugation to remove the cellular debris. Cytokines and chemokines in lungs, spleens, and sera were measured using the Immune Monitoring 48-Plex Mouse ProcartaPlex™ Panel on Curiox DA-Bead DropArray platform according to the manufacturer's instructions. The following analytes were quantified: granulocyte colony-stimulating factor (G-CSF), granulocyte-macrophage colony-stimulating factor (GM-CSF), macrophage colony-stimulating factor (M-CSF), IFN- $\alpha$ , IFN- $\gamma$ , IL-1 $\alpha$ , IL-1 $\beta$ , IL-2, IL-2R, IL-3, IL-4, IL-5, IL-6, IL-7, IL-7Ra, IL-9, IL-10, IL-12p70, IL-13, IL-15, IL-17A, IL-18, IL-19, IL-22, IL-23, IL-25, IL-27, IL-28, IL-31, IL-

33, IL-33R, Leukemia inhibitory factor (LIF), CXCL1, CXCL2, CXCL5, CXCL10, CCL2, CCL3, CCL4, CCL5, CCL7, CCL11, TNF $\alpha$ , receptor activator of nuclear factor kappa-B ligand (RANKL), B-cell activating factor (BAFF), Betacellulin, vascular endothelial growth factor (VEGF)-A, and Leptin. For analyses, the concentration of following analytes remained below the limit of detection at all time points and were excluded: IL-2R, IL-9, IL-19, IL-31, CXCL10, and Leptin in lungs, IL-9 in spleens, and IL-2, IL-3, IL-4, IL-7Ra, IL-13, IL-22, IL-27, LIF, Betacellulin, CXCL5, CCL3, and CCL5 in sera. Cytokine fold changes, i.e., the raw concentrations (pg/ml) relative to the geometric mean concentrations (pg/ml) of mock infected samples, were calculated to control for baseline sex differences.

### **Detection of neutralizing antibodies**

Plasma neutralizing antibodies were detected using microneutralization assay with MDCK cells. Plasma samples were inactivated at 56°C for 30 minutes and 2-fold serial-diluted to neutralize 50 TCID<sub>50</sub> of influenza B virus for 1 hour at room temperature. The plasma-virus mixture was transferred into 96-well tissue-culture plates in quadruplicates and incubated for 24 hours at 32°C to infect MDCK cells. Following incubation, cell culture media were changed to remove the inoculum. Plates were incubated at 32°C for another 5 days, fixed with 4% formaldehyde, and stained with naphthol blue black. The neutralizing antibody titers were calculated as the highest plasma dilution that eliminates the CPE in at least 50% of the wells.

### **Statistical analyses**

Longitudinal morbidity measures, including body mass and temperature, were analyzed with repeated-measures two-way ANOVAs. Longitudinal measures with unmatched samples, including lung virus titers and cytokine fold changes, were analyzed using unmatched two-way

ANOVAs with Bonferroni post hoc correction for multiple comparisons. Single time point neutralizing antibody titers were analyzed using Student t-tests. Comparisons were considered statistically significant at  $p < 0.05$ . All statistical analyses were conducted using Prism 9.



## RESULTS

### **Morbidity from B/Brisbane/60/2008 is greater in males than females**

To investigate sex differences in the outcome of IBV infection, adult male and female C57BL/6 mice were inoculated with  $10^4$  or  $10^5$  TCID<sub>50</sub> of B/Brisbane/60/2008 and were monitored for 15 days for changes in body mass and rectal temperature as well as death (**Figure 1A**). Infection with  $10^4$  TCID<sub>50</sub> did not cause observable disease in either males or females, while infection with  $10^5$  TCID<sub>50</sub> resulted in pathogenesis in both sexes (**Figure 2A and 2B**). Body mass loss was observed after 4-5 days post infection (dpi), and recovery began at 6-7 dpi (**Figure 2A**). Male mice experienced greater morbidity, i.e., had greater body mass loss and [hypothermia](#), compared to the females (**Figure 2A and 2B**,  $p < 0.05$ ). No mortality was observed in female mice, while one male died at 8 dpi among mice infected with  $10^5$  TCID<sub>50</sub>.

### **Male mice have greater titers of B/Brisbane virus in lungs than female mice**

To determine if male biased disease severity was caused by a reduced ability of males to control virus replication, lungs were collected at 1, 3, 5, or 7 dpi for virus titration (**Figure 1B**). A significant main effect of sex was observed, in which lung viral titers peaked in 3 and 5 days after IBV infection, with a consistent trend that males had greater titers than females (**Figure 2C**,  $p < 0.05$ ). There also was a significant interaction between sex and dpi, in which at 5 dpi, the difference of IBV titers in lungs was maximized (**Figure 2C**,  $p < 0.05$ ). These data illustrate that that males compared with females had a reduced ability to control virus replication.

### **Male mice developed an aberrant local inflammatory response**

To understand the possible factors leading to the male bias in pathogenesis and viral clearance, pulmonary, splenic, and peripheral cytokine concentrations were measured at 3 (i.e.,

during peak virus replication) and 7 (i.e., after virus clearance) dpi. Because there can be baseline sex differences associated with instillation of vehicle into the lungs [115], sex difference in the baseline concentrations of cytokines were controlled by analyzing the fold change relative to mock infected male or female mice. In response to B/Brisbane infection, both males and females showed systemic immune activation during the first week after IBV infection, as is reflected in the increased expression of IFN- $\alpha$ , IFN- $\gamma$ , IL-12p70, IL-18, CXCL2, and CXCL5 in the spleen and IFN- $\alpha$ , IL-1 $\beta$ , IL-6, and IL-18 in serum (**Figure 3, Figure 4, and Supplemental Table 1, Supplemental Table 2**). Peripheral induction of cytokines showed rare sex differences. In the spleen, females expressed greater IL-28 than males at 3 dpi, while males expressed greater IL-23 and CXCL10 at 7 dpi (**Figure 3**). In the serum, significant sex differences were only observed at 7 dpi, with greater expression of IL-9, IL-33, CCL7, and CCL11 in females (**Figure 4**).

There were greater differences between males and females at the site of infection (**Figure 5**). At 3 dpi, females presented with greater concentrations of IL-1 $\alpha$ , IL-1 $\beta$ , and IL-12p70 in lungs than males, suggesting that females had a more rapid local innate response during peak virus replication (**Figure 6A, 6B, and 6C,  $p < 0.05$** ). In contrast, at 7 dpi, the pulmonary concentrations of IFN- $\gamma$ , IL-3, IL-6, CCL2, CCL3, and CCL4, were significantly greater in lungs from male than female mice (**Figure 6D, 6E, 6F, 6I, 6J, and 6K,  $p < 0.05$** ). In addition, there was a trend in IFN- $\alpha$  and TNF $\alpha$  that showed greater inductions in females at 3 dpi but in males at 7 dpi (**Figure 6M and 6N**). Taken together, these data suggest that while both males and females experience appropriate immune activation following infection, females develop more rapid cytokine responses in the presence of virus and males sustain cytokine responses after virus has been cleared.

**During the recovery phase of IBV infection, females produced greater neutralizing antibody titers than males**

Recovery from IBV infection requires induction of adaptive immune responses, which contribute to viral clearance and memory responses that protect against re-infection. To evaluate sex differences in the humoral response following IBV infection, serum was collected at 21 dpi from IBV-infected male and female mice (**Figure 1A**). After B/Brisbane infection, female mice produced significantly greater neutralizing antibody titers than male mice (**Figure 7**,  $p < 0.05$ ). The greater neutralizing antibody titers suggest stronger humoral responses in females, which may contribute to the better outcome in females during the primary IBV infection, and provide more efficient protection from the re-exposure to B/Brisbane virus in females than males.

**Figure 1.** Experimental designs.

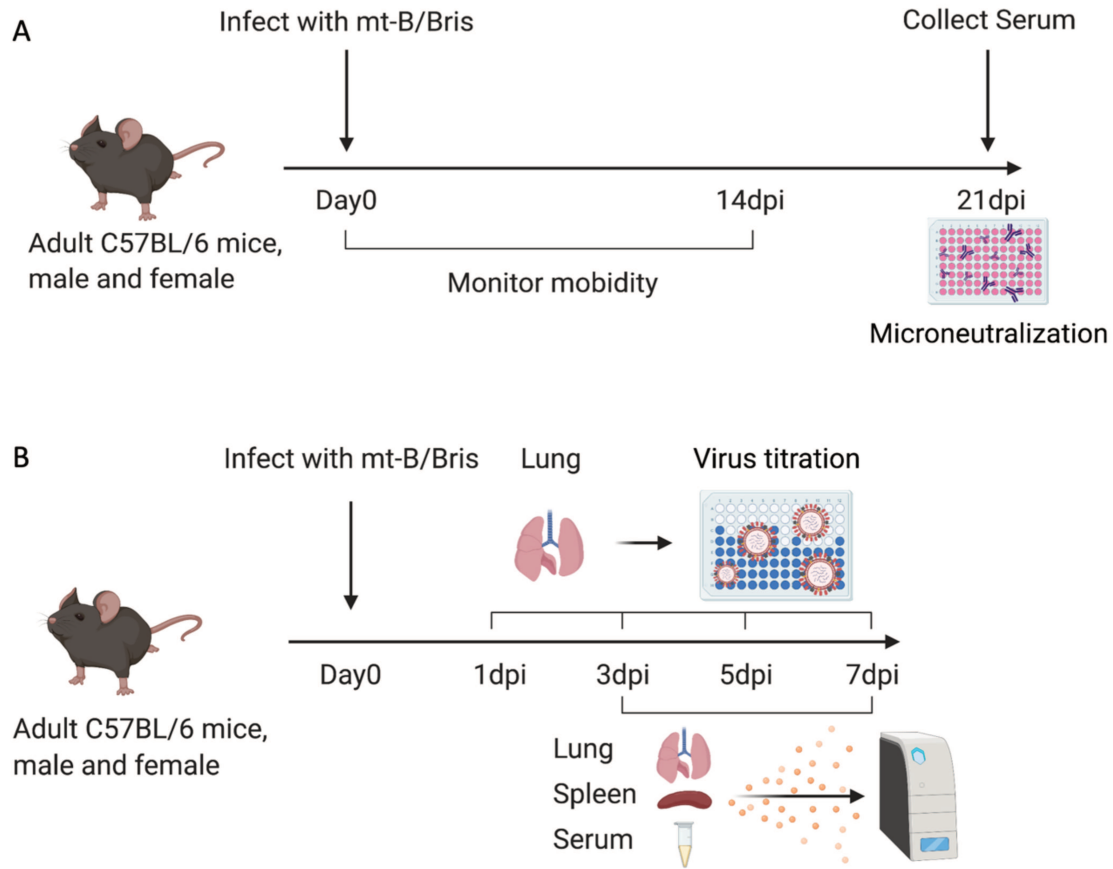


**Figure 2.** Morbidity and lung virus titers of B/Brisbane infected adult male and female C57BL/6 mice.

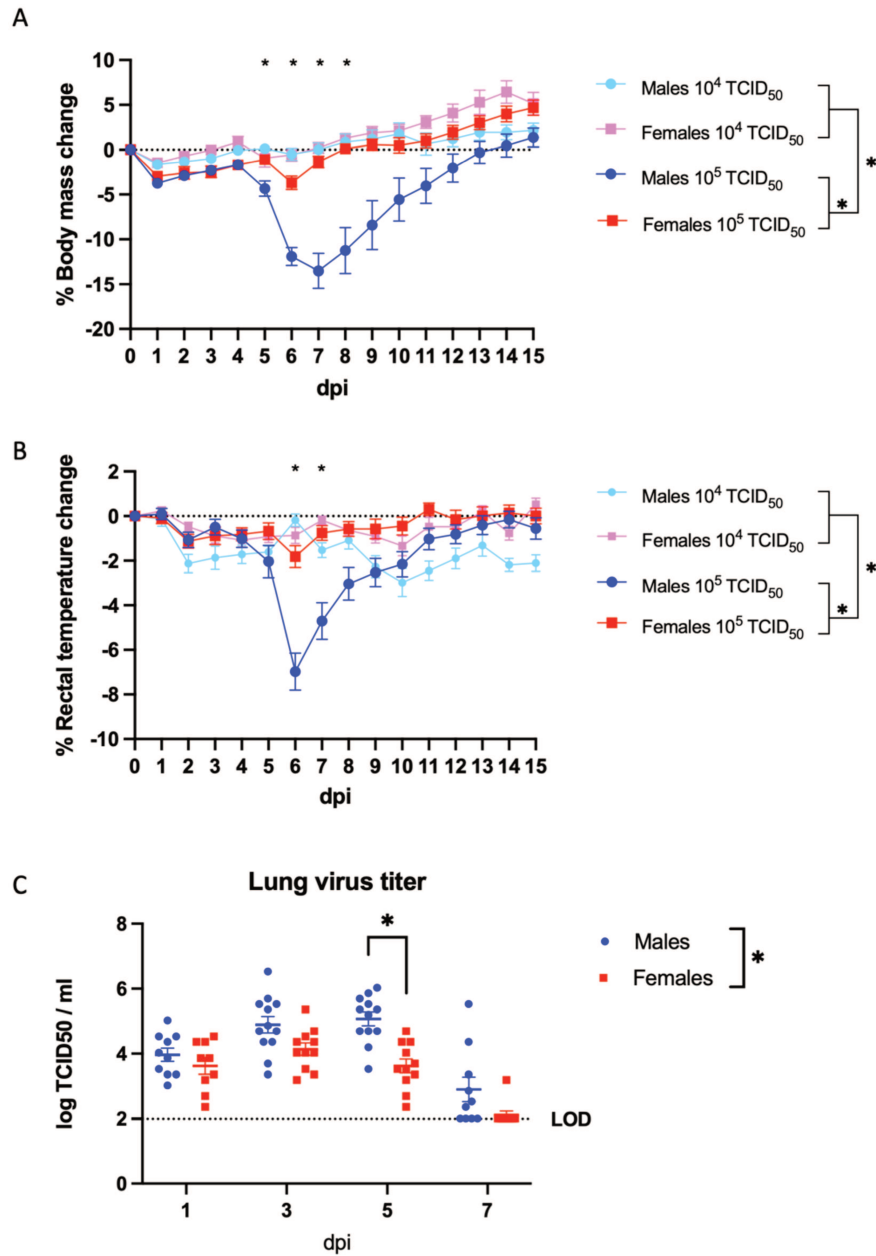
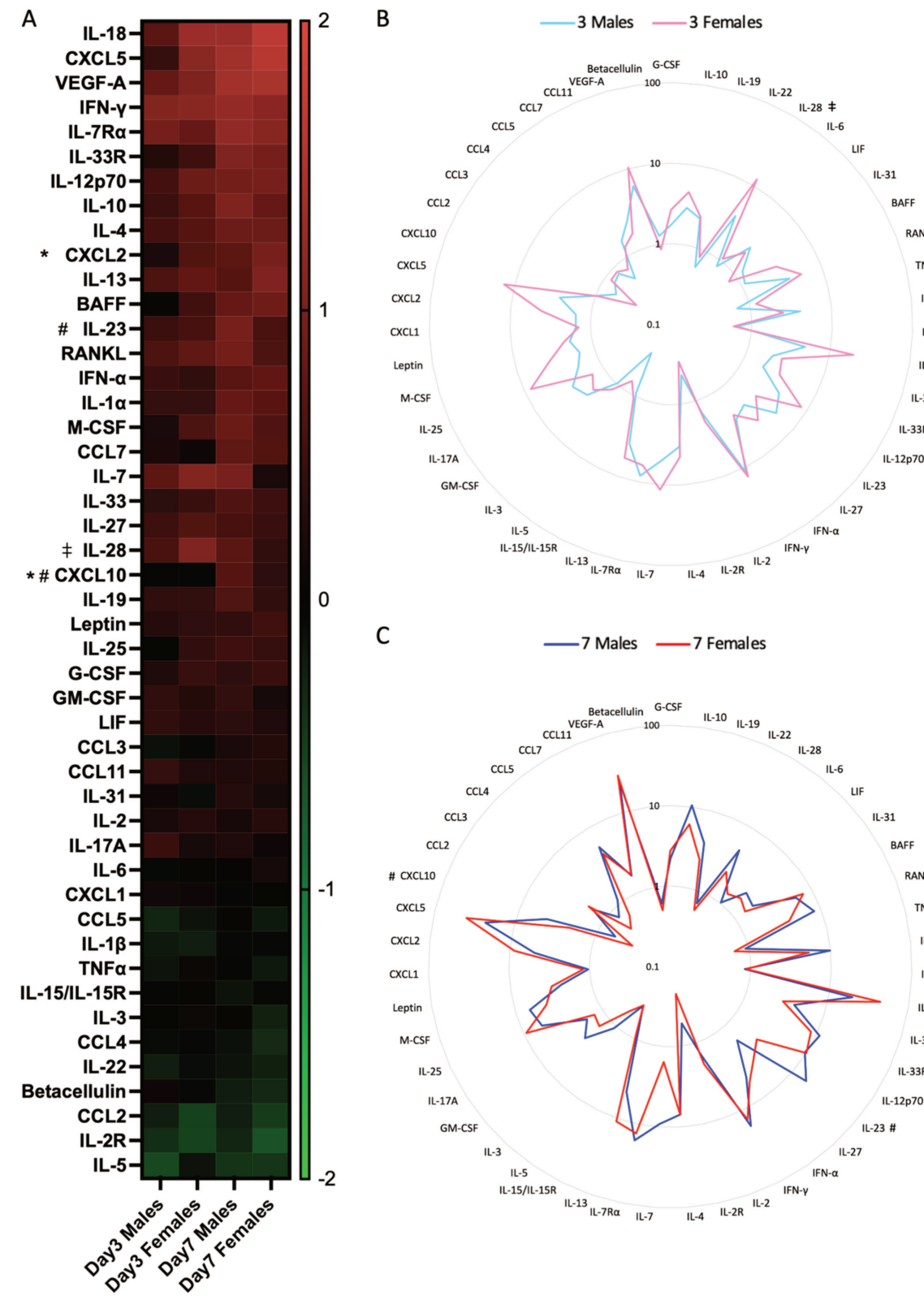
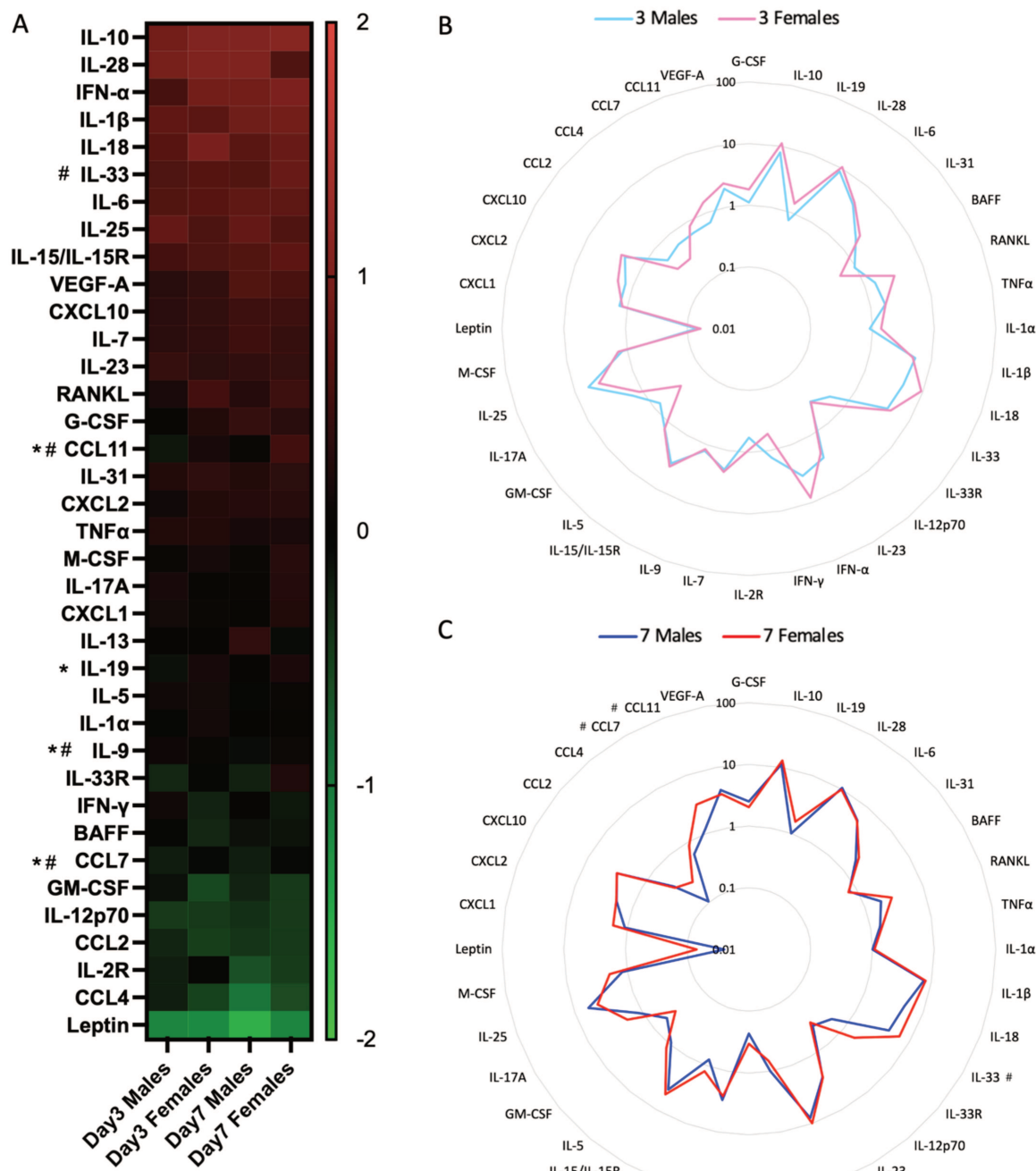


Figure 3. Cytokine fold change profile in spleens.



**Figure 4.** Cytokine fold change profile in sera.



**Figure 5.** Cytokine fold change profile in lungs.

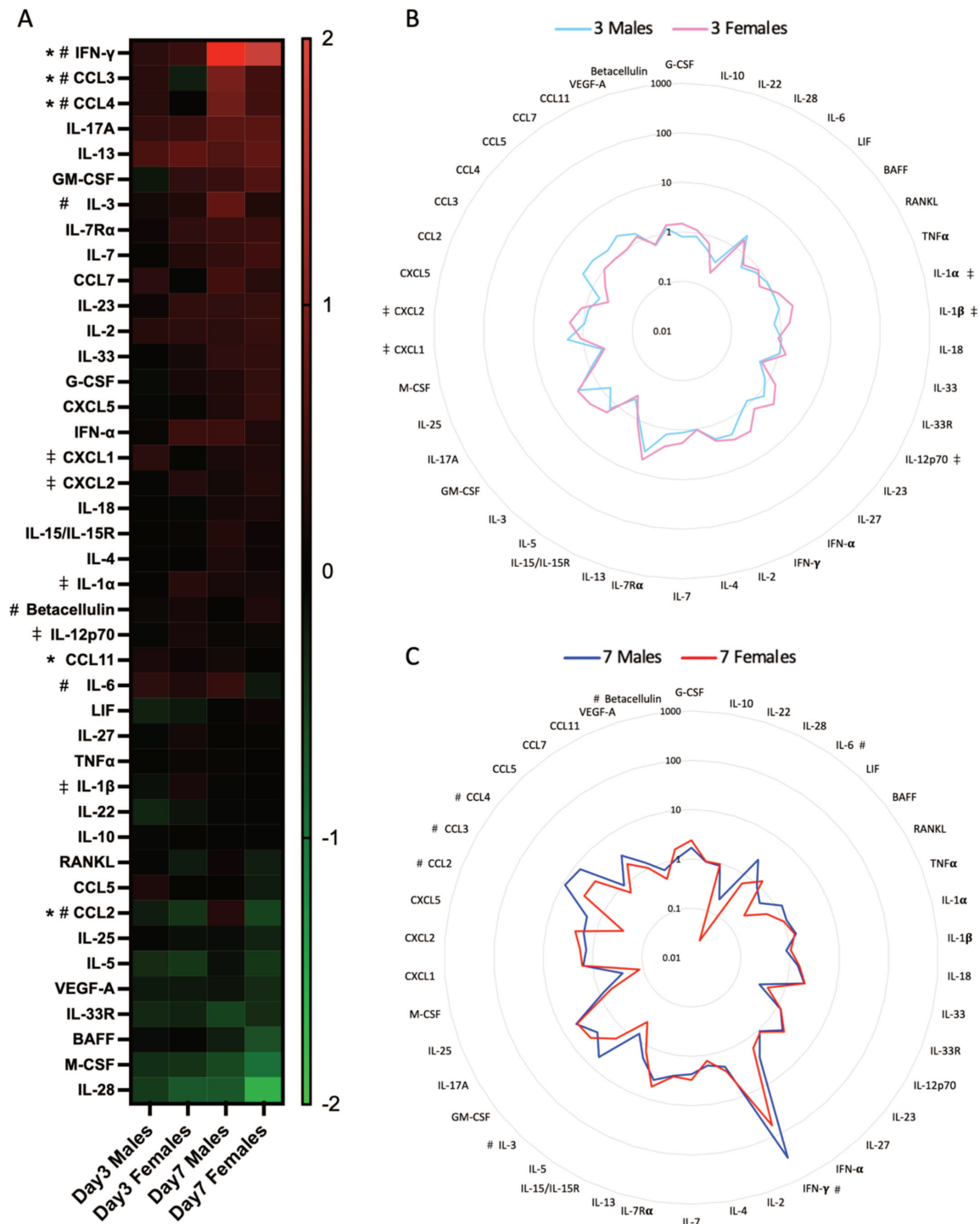




**Figure 6.** Sex difference in the induction of pulmonary cytokines after B/Brisbane infection.

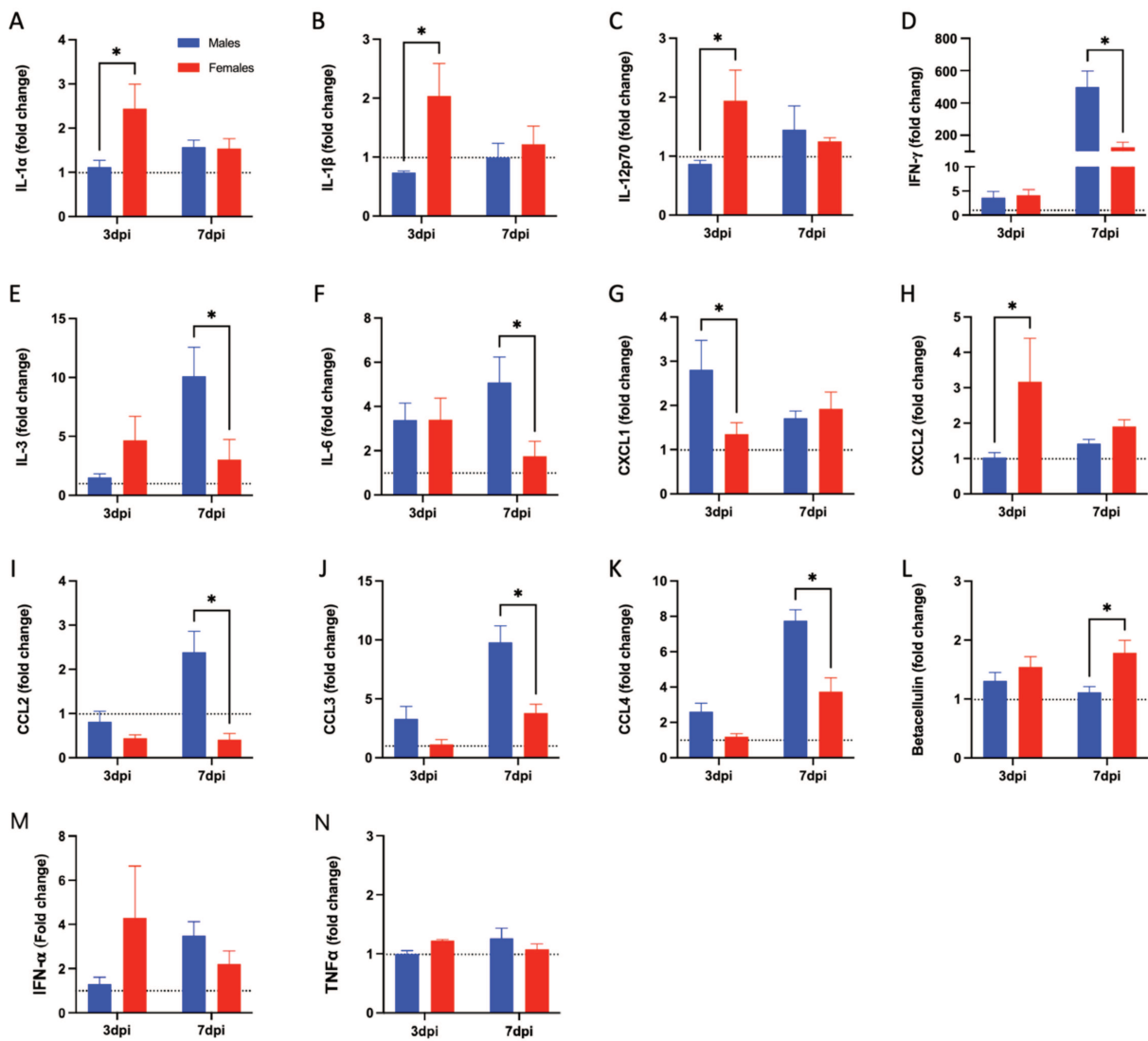
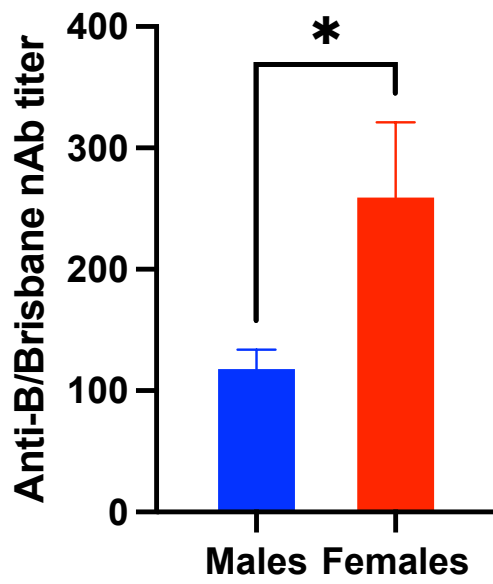


**Figure 7.** Neutralizing antibody titers in the sera at 21 dpi.



## DISCUSSION

In this study, we established a IBV pathogenesis model using adult C57BL/6 mice. Sex differences were observed, with worse symptoms and greater virus replication and slower clearance of virus from the lungs in male mice. Male mice also had slower pulmonary induction of cytokines in the lungs during peak virus replication, but then sustained and even elevated pulmonary cytokine responses after virus had been cleared from the lungs. Females also produced greater antiviral antibody responses than males, which could be significant for protection following re-infection.

Sex biases are observed among many different host species ranging from mice to humans and in response to many pathogens [126]. Generally, the susceptibility to infection is greater for males than females, which could be explained by the sex disparities in gene expression, immune responses, and behavior [127]. Considerable evidence shows that factors associated with biological sex, including sex steroid and growth factor modulation of immune responses, affect IAV pathogenesis (**Table 5**). Sex steroids impact the pathogenesis and outcomes of viral infection by modulating inflammation, antibody production, or tissue repair. However, these mechanisms result in worse outcomes in females following IAV infection, whereas our study showed a male bias in IBV pathogenesis. Therefore, more comprehensive studies are necessary to understand the role of biological sex in the response to IBV infection.

In our study, after the infection of  $10^5$  TCID<sub>50</sub> of B/Brisbane/60/2008, male mice experienced significantly more severe disease than females. Remarkably, the outcomes of IAV infection are generally worse in reproductive aged adult females in both humans and mice, which is opposite to our observation in IBV infection [114, 115, 128, 129]. In fact, a number of studies from our laboratory using diverse H1N1 and H3N2 IAV viruses have shown that adult C57BL/6

female mice experience greater morbidity than male mice (Robinson et al. 2011, Lorenzo et al. 2011, Vermillion et al. 2018). Sex differences in the pathogenesis of IAV are not associated with differences in the ability to control virus replication, because sex differences in pulmonary infectious virus titers have not been observed [114, 115, 129]. Our IBV data, however, show a significant sex effect in pulmonary virus replication kinetics, with male lungs containing higher titers of virus than female lungs.

Innate responses to replicating virus are integral for control of viral infection. During peak viral replication, i.e. at 3 dpi, females had greater concentrations of IL-1 $\alpha$ , IL-1 $\beta$ , and IL-12, which are important for immune responses activation and modulation of T cell differentiation [93, 130-132]. At 7 dpi after B/Bris infection, when the virus had been cleared, males presented with significantly greater concentrations of IFN- $\gamma$ , IL-6, CCL2, CCL3, and CCL4 in lungs compared to females. Noticeably, IFN- $\gamma$ , IL-6, and CCL2 are higher in female lungs than in males after IAV infection [129, 133]. Therefore, the sex difference in the continuous production of IFN- $\gamma$ , IL-6, and CCL2 might be the direct reason for the sex-biased outcome. To test these hypotheses, IFN- $\gamma$  knockout male and female mice should be included in the future work, to see if the sex dimorphisms in viral clearance and in disease outcomes could be neutralized by IFN- $\gamma$  deficiency. IL-6 or CCL2 knockout mice would also help to interpret the mechanisms of sex-biased immunopathogenesis. IFN- $\alpha$  and TNF $\alpha$  also showed a trend in the induction, which was greater in females at 3 dpi, while in males at 7 dpi. The aberrant cytokine induction may result in compromised viral clearance and more severe tissue damage in males.

Successful recovery from influenza infection relies on the immune system to find a balance among antiviral defense, immunopathogenesis, and tissue repair. In our study, at 3 dpi after IBV infection, pro-inflammatory cytokines, including IL-1 $\beta$ , IL-6, and IFN- $\alpha$ , were

increased in serum of both sexes, inducing systematic symptoms such as hypothermia and fatigue[130, 134, 135]. Besides, these cytokines are essential for the activation of immune responses by modulating monocyte differentiation, activating adaptive responses, and promoting antibody isotype switching [73, 131, 136-138]. The antiviral function of IFN family is also important in defense against influenza virus [139]. In lungs, IFN- $\alpha$  and IFN- $\gamma$  were significantly induced to suppress viral replication at 3 dpi. Meanwhile, chemokines were elevated to attract the immune cells to the infection site. However, overproduction of pro-inflammatory cytokines and excessive cytotoxic effects from NK cells and CD8<sup>+</sup> T cells lead to tissue damage[102]. At the end of viral clearance, a downregulation on the expression of pro-inflammatory cytokines and chemokines is inevitable to avoid further damage. At 7 dpi, the levels of IFN- $\gamma$ , IL-6, and CCL2, CCL3, CCL4 in male mice were significantly higher than in female mice, resulting in worse symptoms and longer courses. Interestingly, although IL-6 causes tissue damage, it has been identified to suppress the hyper-inflammation[73]. Therefore, the elevation of IL-6 may serve as a signal for hyper-inflammation. During influenza pathogenesis, IL-12 and IL-33 have been shown to promote tissue repair. We observed higher level of IL-12 in female lungs at 3 dpi, and elevated IL-33 in female serums at 7 dpi, which may contribute to the faster recovery of females.

As IBV is causing greater circulation and diseases, prophylaxis for IBV needs more attention. Males tend to have lower antibody responses than females following influenza vaccination [140-143], which might be attributed to the sex disparity in the global gene expression in B cells [144]. In our study, females produced greater neutralizing antibody titers at 21 dpi after IBV infection, indicating poorer humoral responses to IBV antigens in males, which might be explained by the distinct process of B cell proliferation and differentiation in males and

females. In short, males have lower immunity to IBV antigens but suffer greater diseases from IBV infection. The effects of biological sex on IBV pathogenesis and vaccine responses in humans should be explored. Influenza vaccination rate in males, especially in children and elderly, should be taken seriously.

In summary, our data suggest that males experience more severe disease than females following IBV infection, which may result from impaired viral clearance and compromised innate and adaptive immune responses. To date, studies on IBV pathogenesis are still lacking, and there is no published data comparing male and female responses using animal models. Our study established a successful IBV pathogenic mouse model using mouse-adapted B/Brisbane virus (Victoria lineage) in adult male and female C57BL/6 mice. Other strains of IBV Yamagata lineage, and other mouse strains might be applied to repeat and compare. A comprehensive understanding of IBV pathogenesis in different sexes will help with more precise influenza prophylaxis and treatment. The mechanisms on how sex steroids and sex chromosomal genes regulate the responses to IBV require further investigation. Besides, this study only focused on the sex disparity in reproductive aged adult mice. Juvenile and aged mice should also be included to identify the age-sex interaction in future studies.

**Table 5.** The effect of sex associated factors on influenza pathogenesis.

<b>Factor</b>	<b>Type</b>	<b>Effect</b>	<b>Function</b>
<b>Amphiregulin</b>	Growth factor	Protective	Promote tissue repair
<b>Testosterone</b>	Sex steroid	Protective	Reduce inflammation
<b>Estradiol</b>	Sex steroid	Protective	Reduce inflammation; promote antibody production
<b>Estriol</b>	Sex steroid	Protective	Reduce inflammation
<b>Progesterone</b>	Sex steroid	Protective; harmful	Reduce inflammation; promote tissue repair; reduce adaptive responses

## FIGURE AND TABLE LEGENDS

**Table 1: Structural and functional differences in influenza A (IAV), B (IBV), C (ICV), and D (IDV) viruses.**

**Table 2: Comparison of Victoria and Yamagata lineage influenza B viruses.**

**Table 3: Comparison of the process for IAV transcription and replication.**

**Table 4: Featured cytokines in influenza infection.**

**Table 5: The effect of sex steroids on influenza pathogenesis.**

**Figure 1: Experimental designs.**

(A) Adult male and female C57BL/6 mice were intranasally inoculated with 30 $\mu$ l 10<sup>4</sup> or 10<sup>5</sup> TCID<sub>50</sub> of mouse-adapted B/Brisbane/60/2008 viruses. The mice were then monitored 15 days in body mass and rectal temperature. At 21 days post infection (dpi), mice were euthanized to collect blood for microneutralization assays (n = 10 or 20/group). (B) Adult male and female C57BL/6 mice were intranasally inoculated with 30 $\mu$ l 10<sup>5</sup> TCID<sub>50</sub> of mouse-adapted B/Brisbane/60/2008 viruses. The mice were euthanized at 1, 3, 5, or 7 dpi to collect lung samples for virus titration (n = 9-12/group). At 3 and 7 dpi, mice were euthanized to collect lung, spleen, and serum for cytokine quantification (n = 10-12/group).

**Figure 2: Morbidity and lung virus titers of B/Brisbane infected adult male and female C57BL/6 mice.**

Adult male and female C57BL/6 mice were intranasally inoculated with 30 $\mu$ l 10<sup>4</sup> or 10<sup>5</sup> TCID<sub>50</sub> of mouse-adapted B/Brisbane/60/2008 viruses. Loss of body mass (A) and rectal temperature (B) were measured for 15 days, as correlates of morbidity. Data represents Means  $\pm$  Standard Error of Mean from four groups (n=10 or 20/group). Infectious virus was measured in the lungs by



TCID<sub>50</sub> at 1, 3, 5, or 7 dpi (C; n = 9–12/group/time-point). Significant differences between males and females are denoted by asterisks (\*  $p < 0.05$ ).

**Figure 3: Cytokine fold change profile in spleens.**

Adult male and female C57BL/6 mice were intranasally inoculated with 30μl 10<sup>5</sup> TCID<sub>50</sub> of mouse-adapted B/Brisbane/60/2008 viruses (n = 10-12/group) or mock-infected (n = 9/group).

At 3 and 7 dpi, spleens were harvested and homogenized. The cell-free supernatants were used to quantify 48 cytokine analytes. The color gradient of heatmap (A) represents the log<sub>10</sub> fold change in splenic cytokine concentrations relative to respective mock-infected controls. The radar maps discriminate male and female differences at 3 dpi (B) and 7 dpi (C) in the log<sub>10</sub> fold change of splenic cytokine concentrations relative to respective mock-infected controls. Significant main effects of sex are denoted by asterisks (\*  $p < 0.05$ ). Significant differences between males and females at 3 dpi are denoted by diesis (‡  $p < 0.05$ ). Significant differences between males and females at 7 dpi are denoted by pound (#  $p < 0.05$ ).

**Figure 4: Cytokine fold change profile in sera.**

Adult male and female C57BL/6 mice were intranasally inoculated with 30μl 10<sup>5</sup> TCID<sub>50</sub> of mouse-adapted B/Brisbane/60/2008 viruses (n = 10-12/group) or mock-infected (n = 9/group).

At 3 and 7 dpi, blood was collected, and serum was separated to quantify 48 cytokine analytes.

The color gradient of heatmap (A) represents the log<sub>10</sub> fold change in serum cytokine concentrations relative to respective mock-infected controls. The radar maps discriminate male and female differences at 3 dpi (B) and 7 dpi (C) in the log<sub>10</sub> fold change of cytokine concentrations relative to respective mock-infected controls. Significant main effects of sex are denoted by asterisks (\*  $p < 0.05$ ). Significant differences between males and females at 3 dpi are

denoted by diesis ( $\ddagger p < 0.05$ ). Significant differences between males and females at 7 dpi are denoted by pound ( $\# p < 0.05$ ).

**Figure 5: Cytokine fold change profile in lungs.**

Adult male and female C57BL/6 mice were intranasally inoculated with 30 $\mu$ l 10<sup>5</sup> TCID<sub>50</sub> of mouse-adapted B/Brisbane/60/2008 viruses (n = 10-12/group) or mock-infected (n = 9/group). At 3 and 7 dpi, lungs were harvested and homogenized. The cell-free supernatants were used to quantify 48 cytokine analytes. The color gradient of heatmap (A) represents the log<sub>10</sub> fold change in pulmonary cytokine concentrations relative to respective mock-infected controls. The radar maps discriminate male and female differences at 3 dpi (B) and 7 dpi (C) in the log<sub>10</sub> fold change of cytokine concentrations relative to respective mock-infected controls. Significant main effects of sex are denoted by asterisks ( $* p < 0.05$ ). Significant differences between males and females at 3 dpi are denoted by diesis ( $\ddagger p < 0.05$ ). Significant differences between males and females at 7 dpi are denoted by pound ( $\# p < 0.05$ ).

**Figure 6: Sex difference in the induction of pulmonary cytokines after B/Brisbane infection.**

Adult male and female C57BL/6 mice were intranasally inoculated with 30 $\mu$ l 10<sup>5</sup> TCID<sub>50</sub> of mouse-adapted B/Brisbane/60/2008 viruses (n = 10-12/group) or mock-infected (n = 9/group). At 3 and 7 dpi, lungs were harvested and homogenized. The cell-free lung supernatants were used to quantify 48 cytokine analytes. IFN- $\gamma$  (A), IL-1 $\alpha$  (B), IL-1 $\beta$  (C), IL-3 (D), IL-6 (E), IL-12p70 (F), CXCL1 (G), CXCL2 (H), CCL2 (I), CCL3 (J), CCL4 (K), and Betacellulin (L) showed significant male and female difference in fold change at either 3 dpi or 7 dpi. IFN- $\alpha$  (M) and TNF $\alpha$  (N) showed a trend but without significance. Data represent Means  $\pm$  Standard Error

of Mean of the analytes fold change relative to mock infected mice. Significant differences between males and females are denoted by asterisks (\*  $p < 0.05$ ).

**Figure 7: Neutralizing antibody titers in the serum at 21 dpi.**

Adult male and female C57BL/6 mice were intranasally inoculated with 30 $\mu$ l  $10^5$  TCID<sub>50</sub> of mouse-adapted B/Brisbane/60/2008 viruses (n = 10-12/group). Neutralizing antibody titers were measured at 21 dpi. Significant differences between males and females are denoted by asterisks (\*  $p < 0.05$ ).

## BIBLIOGRAPHY

1. Blanc A, Ruchansky D, Clara M, Achaval F, Le Bas A and Arbiza J (2009) Serologic evidence of influenza A and B viruses in South American fur seals (*Arctocephalus australis*). *J Wildl Dis* 45:519-21. doi: 10.7589/0090-3558-45.2.519
2. Bodewes R, Morick D, de Mutsert G, Osinga N, Bestebroer T, van der Vliet S, Smits SL, Kuiken T, Rimmelzwaan GF, Fouchier RA and Osterhaus AD (2013) Recurring influenza B virus infections in seals. *Emerg Infect Dis* 19:511-2. doi: 10.3201/eid1903.120965
3. Ohishi K, Ninomiya A, Kida H, Park CH, Maruyama T, Arai T, Katsumata E, Tobayama T, Boltunov AN, Khuraskin LS and Miyazaki N (2002) Serological evidence of transmission of human influenza A and B viruses to Caspian seals (*Phoca caspica*). *Microbiol Immunol* 46:639-44. doi: 10.1111/j.1348-0421.2002.tb02746.x
4. Osterhaus ADME, Rimmelzwaan GF, Martina BEE, Bestebroer TM and Fouchier RAM (2000) Influenza B Virus in Seals. *Science* 288:1051-1053. doi: 10.1126/science.288.5468.1051
5. Francis T, Quilligan JJ and Minuse E (1950) Identification of Another Epidemic Respiratory Disease. *Science* 112:495. doi: 10.1126/science.112.2913.495
6. Taylor RM (1949) Studies on survival of influenza virus between epidemics and antigenic variants of the virus. *Am J Public Health Nations Health* 39:171-8. doi: 10.2105/ajph.39.2.171
7. Taylor RM (1951) A further note on 1233 influenza C virus. *Arch Gesamte Virusforsch* 4:485-500. doi: 10.1007/bf01241168
8. Dykes AC, Cherry JD and Nolan CE (1980) A Clinical, Epidemiologic, Serologic, and Virologic Study of Influenza C Virus Infection. *Archives of Internal Medicine* 140:1295-1298. doi: 10.1001/archinte.1980.00330210043021
9. Homma M, Ohyama S and Katagiri S (1982) Age distribution of the antibody to type C influenza virus. *Microbiol Immunol* 26:639-42. doi: 10.1111/mim.1982.26.7.639
10. O'Callaghan RJ, Gohd RS and Labat DD (1980) Human antibody to influenza C virus: its age-related distribution and distinction from receptor analogs. *Infect Immun* 30:500-5.
11. Hause BM, Ducatez M, Collin EA, Ran Z, Liu R, Sheng Z, Armien A, Kaplan B, Chakravarty S, Hoppe AD, Webby RJ, Simonson RR and Li F (2013) Isolation of a novel swine influenza virus from Oklahoma in 2011 which is distantly related to human influenza C viruses. *PLoS Pathog* 9:e1003176. doi: 10.1371/journal.ppat.1003176
12. Hause BM, Collin EA, Liu R, Huang B, Sheng Z, Lu W, Wang D, Nelson EA and Li F (2014) Characterization of a novel influenza virus in cattle and Swine: proposal for a new genus in the Orthomyxoviridae family. *mBio* 5:e00031-14. doi: 10.1128/mBio.00031-14
13. Rota PA, Wallis TR, Harmon MW, Rota JS, Kendal AP and Nerome K (1990) Cocirculation of two distinct evolutionary lineages of influenza type B virus since 1983. *Virology* 175:59-68. doi: 10.1016/0042-6822(90)90186-U
14. Matsuzaki Y, Sugawara K, Furuse Y, Shimotai Y, Hongo S, Oshitani H, Mizuta K and Nishimura H (2016) Genetic Lineage and Reassortment of Influenza C Viruses Circulating between 1947 and 2014. *Journal of Virology* 90:8251. doi: 10.1128/JVI.00969-16
15. Murakami S, Sato R, Ishida H, Katayama M, Takenaka-Uema A and Horimoto T (2020) Influenza D Virus of New Phylogenetic Lineage, Japan. *Emerg Infect Dis* 26:168-171. doi: 10.3201/eid2601.191092

16. Steinhauer DA, Domingo E and Holland JJ (1992) Lack of evidence for proofreading mechanisms associated with an RNA virus polymerase. *Gene* 122:281-288. doi: [https://doi.org/10.1016/0378-1119\(92\)90216-C](https://doi.org/10.1016/0378-1119(92)90216-C)
17. McCullers JA, Saito T and Iverson AR (2004) Multiple genotypes of influenza B virus circulated between 1979 and 2003. *Journal of virology* 78:12817-12828. doi: 10.1128/JVI.78.23.12817-12828.2004
18. Chen R and Holmes EC (2008) The evolutionary dynamics of human influenza B virus. *Journal of molecular evolution* 66:655-663. doi: 10.1007/s00239-008-9119-z
19. Cox NJ and Bender CA (1995) The molecular epidemiology of influenza viruses. *Seminars in Virology* 6:359-370. doi: [https://doi.org/10.1016/S1044-5773\(05\)80013-7](https://doi.org/10.1016/S1044-5773(05)80013-7)
20. Xu X, Lindstrom SE, Shaw MW, Smith CB, Hall HE, Mungall BA, Subbarao K, Cox NJ and Klimov A (2004) Reassortment and evolution of current human influenza A and B viruses. *Virus Research* 103:55-60. doi: <https://doi.org/10.1016/j.virusres.2004.02.013>
21. Baker SF, Nogales A, Finch C, Tuffy KM, Domm W, Perez DR, Topham DJ and Martínez-Sobrido L (2014) Influenza A and B virus intertypic reassortment through compatible viral packaging signals. *Journal of virology* 88:10778-10791. doi: 10.1128/JVI.01440-14
22. Centers for Disease Control and Prevention (CDC) (2018) Past Pandemics. <https://www.cdc.gov/flu/pandemic-resources/basics/past-pandemics.html>
23. Centers for Disease Control and Prevention (CDC) (2019) 1968 Pandemic (H3N2 virus). <https://www.cdc.gov/flu/pandemic-resources/1968-pandemic.html>
24. Centers for Disease Control and Prevention (CDC) (2019) 2009 H1N1 Pandemic (H1N1pdm09 virus). <https://www.cdc.gov/flu/pandemic-resources/2009-h1n1-pandemic.html>
25. Caini S, Kuszniarz G, Garate VV, Wangchuk S, Thapa B, de Paula Junior FJ, Ferreira de Almeida WA, Njouom R, Fasce RA, Bustos P, Feng L, Peng Z, Araya JL, Bruno A, de Mora D, Barahona de Gamez MJ, Pebody R, Zambon M, Higueros R, Rivera R, Kosasih H, Castrucci MR, Bella A, Kadjo HA, Daouda C, Makusheva A, Bessonova O, Chaves SS, Emukule GO, Heraud JM, Razanajatovo NH, Barakat A, El Falaki F, Meijer A, Donker GA, Huang QS, Wood T, Balmaseda A, Palekar R, Arevalo BM, Rodrigues AP, Guimar R, Lee VJM, Ang LW, Cohen C, Treurnicht F, Mironenko A, Holubka O, Bresee J, Brammer L, Le MTQ, Hoang PVM, El Guerche-Seblain C, Paget J and Global Influenza BSt (2019) The epidemiological signature of influenza B virus and its B/Victoria and B/Yamagata lineages in the 21st century. *PLoS One* 14:e0222381. doi: 10.1371/journal.pone.0222381
26. Virk RK, Jayakumar J, Mendenhall IH, Moorthy M, Lam P, Linster M, Lim J, Lin C, Oon LLE, Lee HK, Koay ESC, Vijaykrishna D, Smith GJD and Su YCF (2020) Divergent evolutionary trajectories of influenza B viruses underlie their contemporaneous epidemic activity. *Proc Natl Acad Sci U S A* 117:619-628. doi: 10.1073/pnas.1916585116
27. Cowling BJ, Wu P, Lo JYC, Chan KH, Chan ELY, Fang VJ, So LY, Peiris JSM and Chiu SS (2017) Population-Based Pediatric Hospitalization Burden of Lineage-Specific Influenza B in Hong Kong, 2004-2014. *Clin Infect Dis* 65:300-307. doi: 10.1093/cid/cix312
28. World Health Organization (WHO) (2020) Influenza (seasonal). [https://www.who.int/en/news-room/fact-sheets/detail/influenza-\(seasonal\)](https://www.who.int/en/news-room/fact-sheets/detail/influenza-(seasonal))
29. Centers for Disease Control and Prevention (CDC) (2021) Age Group Distribution of Influenza Positive Specimens Reported by Public Health Laboratories, National Summary. [https://gis.cdc.gov/grasp/fluview/flu\\_by\\_age\\_virus.html](https://gis.cdc.gov/grasp/fluview/flu_by_age_virus.html)
30. Centers for Disease Control and Prevention (CDC) (2021) Influenza-Associated Pediatric Mortality. <https://gis.cdc.gov/GRASP/Fluview/PedFluDeath.html>

31. Ito T, Suzuki Y, Takada A, Kawamoto A, Otsuki K, Masuda H, Yamada M, Suzuki T, Kida H and Kawaoka Y (1997) Differences in sialic acid-galactose linkages in the chicken egg amnion and allantois influence human influenza virus receptor specificity and variant selection. *Journal of virology* 71:3357-3362. doi: 10.1128/JVI.71.4.3357-3362.1997
32. Ryan-Poirier K, Suzuki Y, Bean WJ, Kobasa D, Takada A, Ito T and Kawaoka Y (1998) Changes in H3 influenza A virus receptor specificity during replication in humans. *Virus Research* 56:169-176. doi: [https://doi.org/10.1016/S0168-1702\(98\)00067-7](https://doi.org/10.1016/S0168-1702(98)00067-7)
33. Kida H, Yanagawa R and Matsuoka Y (1980) Duck influenza lacking evidence of disease signs and immune response. *Infection and immunity* 30:547-553.
34. Ito T, Couceiro JN, Kelm S, Baum LG, Krauss S, Castrucci MR, Donatelli I, Kida H, Paulson JC, Webster RG and Kawaoka Y (1998) Molecular basis for the generation in pigs of influenza A viruses with pandemic potential. *Journal of virology* 72:7367-7373. doi: 10.1128/JVI.72.9.7367-7373.1998
35. Shinya K, Ebina M, Yamada S, Ono M, Kasai N and Kawaoka Y (2006) Avian flu: influenza virus receptors in the human airway. *Nature* 440:435-6. doi: 10.1038/440435a
36. Sriwilaijaroen N and Suzuki Y (2012) Molecular basis of the structure and function of H1 hemagglutinin of influenza virus. *Proc Jpn Acad Ser B Phys Biol Sci* 88:226-49. doi: 10.2183/pjab.88.226
37. Pinto LH, Holsinger LJ and Lamb RA (1992) Influenza virus M2 protein has ion channel activity. *Cell* 69:517-528. doi: [https://doi.org/10.1016/0092-8674\(92\)90452-I](https://doi.org/10.1016/0092-8674(92)90452-I)
38. Eisefeld AJ, Neumann G and Kawaoka Y (2015) At the centre: influenza A virus ribonucleoproteins. *Nat Rev Microbiol* 13:28-41. doi: 10.1038/nrmicro3367
39. Barrett T, Wolstenholme AJ and Mahy BW (1979) Transcription and replication of influenza virus RNA. *Virology* 98:211-25. doi: 10.1016/0042-6822(79)90539-7
40. Neumann G, Brownlee GG, Fodor E and Kawaoka Y (2004) Orthomyxovirus Replication, Transcription, and Polyadenylation. In: Kawaoka Y (ed) *Biology of Negative Strand RNA Viruses: The Power of Reverse Genetics*, Springer Berlin Heidelberg, Berlin, Heidelberg pp. 121-143
41. Pflug A, Lukarska M, Resa-Infante P, Reich S and Cusack S (2017) Structural insights into RNA synthesis by the influenza virus transcription-replication machine. *Virus Research* 234:103-117. doi: <https://doi.org/10.1016/j.virusres.2017.01.013>
42. Mogensen TH (2009) Pathogen recognition and inflammatory signaling in innate immune defenses. *Clin Microbiol Rev* 22:240-73, Table of Contents. doi: 10.1128/cmr.00046-08
43. Iwasaki A and Pillai PS (2014) Innate immunity to influenza virus infection. *Nat Rev Immunol* 14:315-28. doi: 10.1038/nri3665
44. Le Goffic R, Balloy V, Lagranderie M, Alexopoulou L, Escriou N, Flavell R, Chignard M and Si-Tahar M (2006) Detrimental contribution of the Toll-like receptor (TLR)3 to influenza A virus-induced acute pneumonia. *PLoS Pathog* 2:e53. doi: 10.1371/journal.ppat.0020053
45. Guillot L, Le Goffic R, Bloch S, Escriou N, Akira S, Chignard M and Si-Tahar M (2005) Involvement of toll-like receptor 3 in the immune response of lung epithelial cells to double-stranded RNA and influenza A virus. *J Biol Chem* 280:5571-80. doi: 10.1074/jbc.M410592200
46. Le Goffic R, Pothlichet J, Vitour D, Fujita T, Meurs E, Chignard M and Si-Tahar M (2007) Cutting Edge: Influenza A virus activates TLR3-dependent inflammatory and RIG-I-dependent antiviral responses in human lung epithelial cells. *J Immunol* 178:3368-72. doi: 10.4049/jimmunol.178.6.3368

47. Lee AJ and Ashkar AA (2018) The Dual Nature of Type I and Type II Interferons. *Frontiers in Immunology* 9. doi: 10.3389/fimmu.2018.02061
48. García-Sastre A (2011) Induction and evasion of type I interferon responses by influenza viruses. *Virus research* 162:12-18. doi: 10.1016/j.virusres.2011.10.017
49. Brydon EWA, Morris SJ and Sweet C (2005) Role of apoptosis and cytokines in influenza virus morbidity. *FEMS Microbiology Reviews* 29:837-850. doi: 10.1016/j.femsre.2004.12.003
50. Manetti R, Parronchi P, Giudizi MG, Piccinini MP, Maggi E, Trinchieri G and Romagnani S (1993) Natural killer cell stimulatory factor (interleukin 12 [IL-12]) induces T helper type 1 (Th1)-specific immune responses and inhibits the development of IL-4-producing Th cells. *The Journal of experimental medicine* 177:1199-1204. doi: 10.1084/jem.177.4.1199
51. Heer AK, Shamshiev A, Donda A, Uematsu S, Akira S, Kopf M and Marsland BJ (2007) TLR signaling fine-tunes anti-influenza B cell responses without regulating effector T cell responses. *J Immunol* 178:2182-91. doi: 10.4049/jimmunol.178.4.2182
52. Pone EJ, Lou Z, Lam T, Greenberg ML, Wang R, Xu Z and Casali P (2015) B cell TLR1/2, TLR4, TLR7 and TLR9 interact in induction of class switch DNA recombination: modulation by BCR and CD40, and relevance to T-independent antibody responses. *Autoimmunity* 48:1-12. doi: 10.3109/08916934.2014.993027
53. Jeisy-Scott V, Kim JH, Davis WG, Cao W, Katz JM and Sambhara S (2012) TLR7 recognition is dispensable for influenza virus A infection but important for the induction of hemagglutinin-specific antibodies in response to the 2009 pandemic split vaccine in mice. *J Virol* 86:10988-98. doi: 10.1128/JVI.01064-12
54. To EE, Erlich J, Liong F, Luong R, Liong S, Bozinovski S, Seow HJ, O'Leary JJ, Brooks DA, Vlahos R and Selemidis S (2019) Intranasal and epicutaneous administration of Toll-like receptor 7 (TLR7) agonists provides protection against influenza A virus-induced morbidity in mice. *Sci Rep* 9:2366. doi: 10.1038/s41598-019-38864-5
55. Pichlmair A, Schulz O, Tan CP, Näslund TI, Liljeström P, Weber F and Reis e Sousa C (2006) RIG-I-Mediated Antiviral Responses to Single-Stranded RNA Bearing 5'-Phosphates. *Science* 314:997-1001. doi: 10.1126/science.1132998
56. Hornung V, Ellegast J, Kim S, Brzózka K, Jung A, Kato H, Poeck H, Akira S, Conzelmann K-K, Schlee M, Endres S and Hartmann G (2006) 5'-Triphosphate RNA Is the Ligand for RIG-I. *Science* 314:994-997. doi: 10.1126/science.1132505
57. Rehwinkel J, Tan CP, Goubau D, Schulz O, Pichlmair A, Bier K, Robb N, Vreede F, Barclay W, Fodor E and Reis e Sousa C (2010) RIG-I detects viral genomic RNA during negative-strand RNA virus infection. *Cell* 140:397-408. doi: 10.1016/j.cell.2010.01.020
58. Seth RB, Sun L, Ea CK and Chen ZJ (2005) Identification and characterization of MAVS, a mitochondrial antiviral signaling protein that activates NF-kappaB and IRF 3. *Cell* 122:669-82. doi: 10.1016/j.cell.2005.08.012
59. Kuriakose T and Kanneganti TD (2017) Regulation and functions of NLRP3 inflammasome during influenza virus infection. *Mol Immunol* 86:56-64. doi: 10.1016/j.molimm.2017.01.023
60. Swanson KV, Deng M and Ting JPY (2019) The NLRP3 inflammasome: molecular activation and regulation to therapeutics. *Nature Reviews Immunology* 19:477-489. doi: 10.1038/s41577-019-0165-0

61. Ichinohe T, Lee HK, Ogura Y, Flavell R and Iwasaki A (2009) Inflammasome recognition of influenza virus is essential for adaptive immune responses. *The Journal of experimental medicine* 206:79-87. doi: 10.1084/jem.20081667
62. Centers for Disease Control and Prevention (CDC) (2020) Flu Symptoms & Complications. <https://www.cdc.gov/flu/symptoms/symptoms.htm>
63. Szretter KJ, Gangappa S, Lu X, Smith C, Shieh W-J, Zaki SR, Sambhara S, Tumpey TM and Katz JM (2007) Role of Host Cytokine Responses in the Pathogenesis of Avian H5N1 Influenza Viruses in Mice. *Journal of Virology* 81:2736-2744. doi: 10.1128/jvi.02336-06
64. Peper RL and Van Campen H (1995) Tumor necrosis factor as a mediator of inflammation in influenza A viral pneumonia. *Microbial Pathogenesis* 19:175-183. doi: <https://doi.org/10.1006/mpat.1995.0056>
65. Hussell T, Pennycook A and Openshaw PJM (2001) Inhibition of tumor necrosis factor reduces the severity of virus-specific lung immunopathology. *European Journal of Immunology* 31:2566-2573. doi: [https://doi.org/10.1002/1521-4141\(200109\)31:9<2566::AID-IMMU2566>3.0.CO;2-L](https://doi.org/10.1002/1521-4141(200109)31:9<2566::AID-IMMU2566>3.0.CO;2-L)
66. Hall JC and Rosen A (2010) Type I interferons: crucial participants in disease amplification in autoimmunity. *Nat Rev Rheumatol* 6:40-9. doi: 10.1038/nrrheum.2009.237
67. Isaacs A and Lindenmann J (1957) Virus interference. I. The interferon. *Proc R Soc Lond B Biol Sci* 147:258-67. doi: 10.1098/rspb.1957.0048
68. Liu Q, Zhou YH and Yang ZQ (2016) The cytokine storm of severe influenza and development of immunomodulatory therapy. *Cell Mol Immunol* 13:3-10. doi: 10.1038/cmi.2015.74
69. Davidson S, Crotta S, McCabe TM and Wack A (2014) Pathogenic potential of interferon alphabeta in acute influenza infection. *Nat Commun* 5:3864. doi: 10.1038/ncomms4864
70. Schmitz N, Kurrer M, Bachmann MF and Kopf M (2005) Interleukin-1 Is Responsible for Acute Lung Immunopathology but Increases Survival of Respiratory Influenza Virus Infection. *Journal of Virology* 79:6441-6448. doi: 10.1128/jvi.79.10.6441-6448.2005
71. Tate MD, Ong JDH, Dowling JK, McAuley JL, Robertson AB, Latz E, Drummond GR, Cooper MA, Hertzog PJ and Mansell A (2016) Reassessing the role of the NLRP3 inflammasome during pathogenic influenza A virus infection via temporal inhibition. *Sci Rep* 6:27912. doi: 10.1038/srep27912
72. Dienz O, Rud JG, Eaton SM, Lanthier PA, Burg E, Drew A, Bunn J, Suratt BT, Haynes L and Rincon M (2012) Essential role of IL-6 in protection against H1N1 influenza virus by promoting neutrophil survival in the lung. *Mucosal Immunology* 5:258-266. doi: 10.1038/mi.2012.2
73. Lauder SN, Jones E, Smart K, Bloom A, Williams AS, Hindley JP, Ondondo B, Taylor PR, Clement M, Fielding C, Godkin AJ, Jones SA and Gallimore AM (2013) Interleukin-6 limits influenza-induced inflammation and protects against fatal lung pathology. *European journal of immunology* 43:2613-2625. doi: 10.1002/eji.201243018
74. Tisoncik JR, Korth MJ, Simmons CP, Farrar J, Martin TR and Katze MG (2012) Into the eye of the cytokine storm. *Microbiol Mol Biol Rev* 76:16-32. doi: 10.1128/MMBR.05015-11
75. Krammer F (2019) The human antibody response to influenza A virus infection and vaccination. *Nat Rev Immunol* 19:383-397. doi: 10.1038/s41577-019-0143-6
76. Bahadoran A, Lee SH, Wang SM, Manikam R, Rajarajeswaran J, Raju CS and Sekaran SD (2016) Immune Responses to Influenza Virus and Its Correlation to Age and Inherited Factors. *Frontiers in Microbiology* 7. doi: 10.3389/fmicb.2016.01841



77. Huber VC, Lynch JM, Bucher DJ, Le J and Metzger DW (2001) Fc Receptor-Mediated Phagocytosis Makes a Significant Contribution to Clearance of Influenza Virus Infections. *The Journal of Immunology* 166:7381-7388. doi: 10.4049/jimmunol.166.12.7381
78. Throsby M, van den Brink E, Jongeneelen M, Poon LLM, Alard P, Cornelissen L, Bakker A, Cox F, van Deventer E, Guan Y, Cinatl J, ter Meulen J, Lasters I, Carsetti R, Peiris M, de Kruif J and Goudsmit J (2008) Heterosubtypic neutralizing monoclonal antibodies cross-protective against H5N1 and H1N1 recovered from human IgM<sup>+</sup> memory B cells. *PloS one* 3:e3942-e3942. doi: 10.1371/journal.pone.0003942
79. Ekiert DC and Wilson IA (2012) Broadly neutralizing antibodies against influenza virus and prospects for universal therapies. *Current opinion in virology* 2:134-141. doi: 10.1016/j.coviro.2012.02.005
80. DiLillo DJ, Tan GS, Palese P and Ravetch JV (2014) Broadly neutralizing hemagglutinin stalk-specific antibodies require FcγR interactions for protection against influenza virus in vivo. *Nature medicine* 20:143-151. doi: 10.1038/nm.3443
81. Dreyfus C, Laursen NS, Kwaks T, Zuijdgeest D, Khayat R, Ekiert DC, Lee JH, Metlagel Z, Bujny MV, Jongeneelen M, van der Vlugt R, Lamrani M, Korse HJWM, Geelen E, Sahin Ö, Sieuwerts M, Brakenhoff JPJ, Vogels R, Li OTW, Poon LLM, Peiris M, Koudstaal W, Ward AB, Wilson IA, Goudsmit J and Friesen RHE (2012) Highly Conserved Protective Epitopes on Influenza B Viruses. *Science* 337:1343-1348. doi: 10.1126/science.1222908
82. Corti D, Voss J, Gamblin SJ, Codoni G, Macagno A, Jarrossay D, Vachieri SG, Pinna D, Minola A, Vanzetta F, Silacci C, Fernandez-Rodriguez BM, Agatic G, Bianchi S, Giacchetto-Sasselli I, Calder L, Sallusto F, Collins P, Haire LF, Temperton N, Langedijk JPM, Skehel JJ and Lanzavecchia A (2011) A Neutralizing Antibody Selected from Plasma Cells That Binds to Group 1 and Group 2 Influenza A Hemagglutinins. *Science* 333:850-856. doi: 10.1126/science.1205669
83. Sui J, Hwang WC, Perez S, Wei G, Aird D, Chen L-m, Santelli E, Stec B, Cadwell G, Ali M, Wan H, Murakami A, Yammanuru A, Han T, Cox NJ, Bankston LA, Donis RO, Liddington RC and Marasco WA (2009) Structural and functional bases for broad-spectrum neutralization of avian and human influenza A viruses. *Nature Structural & Molecular Biology* 16:265-273. doi: 10.1038/nsmb.1566
84. Ekiert DC, Bhabha G, Elsliger M-A, Friesen RHE, Jongeneelen M, Throsby M, Goudsmit J and Wilson IA (2009) Antibody Recognition of a Highly Conserved Influenza Virus Epitope. *Science* 324:246-251. doi: 10.1126/science.1171491
85. Ekiert DC, Friesen RHE, Bhabha G, Kwaks T, Jongeneelen M, Yu W, Ophorst C, Cox F, Korse HJWM, Brandenburg B, Vogels R, Brakenhoff JPJ, Kompier R, Koldijk MH, Cornelissen LAHM, Poon LLM, Peiris M, Koudstaal W, Wilson IA and Goudsmit J (2011) A Highly Conserved Neutralizing Epitope on Group 2 Influenza A Viruses. *Science* 333:843-850. doi: 10.1126/science.1204839
86. Stadlbauer D, Zhu X, McMahon M, Turner JS, Wohlbold TJ, Schmitz AJ, Strohmeier S, Yu W, Nachbagauer R, Mudd PA, Wilson IA, Ellebedy AH and Krammer F (2019) Broadly protective human antibodies that target the active site of influenza virus neuraminidase. *Science* 366:499-504. doi: 10.1126/science.aay0678
87. Chen Y-Q, Wohlbold TJ, Zheng N-Y, Huang M, Huang Y, Neu KE, Lee J, Wan H, Rojas KT, Kirkpatrick E, Henry C, Palm A-KE, Stamper CT, Lan LY-L, Topham DJ, Treanor J, Wrammert J, Ahmed R, Eichelberger MC, Georgiou G, Krammer F and Wilson PC (2018)

- Influenza Infection in Humans Induces Broadly Cross-Reactive and Protective Neuraminidase-Reactive Antibodies. *Cell* 173:417-429.e10. doi: <https://doi.org/10.1016/j.cell.2018.03.030>
88. De Boer GF, Back W and Osterhaus DME (1990) A ELISA for detection of antibodies against influenza A nucleoprotein in humans and various animal species. *Archives of virology* 115:47-61.
  89. Cretescu L, Beare AS and Schild GC (1978) Formation of antibody to matrix protein in experimental human influenza A virus infections. *Infection and immunity* 22:322-327. doi: 10.1128/IAI.22.2.322-327.1978
  90. Grandea AG, 3rd, Olsen OA, Cox TC, Renshaw M, Hammond PW, Chan-Hui P-Y, Mitcham JL, Cieplak W, Stewart SM, Grantham ML, Pekosz A, Kiso M, Shinya K, Hatta M, Kawaoka Y and Moyle M (2010) Human antibodies reveal a protective epitope that is highly conserved among human and nonhuman influenza A viruses. *Proceedings of the National Academy of Sciences of the United States of America* 107:12658-12663. doi: 10.1073/pnas.0911806107
  91. Renegar KB, Small PA, Jr., Boykins LG and Wright PF (2004) Role of IgA versus IgG in the control of influenza viral infection in the murine respiratory tract. *J Immunol* 173:1978-86. doi: 10.4049/jimmunol.173.3.1978
  92. Rothbarth PH, Groen J, Bohnen AM, de Groot R and Osterhaus ADME (1999) Influenza virus serology—a comparative study. *Journal of Virological Methods* 78:163-169. doi: [https://doi.org/10.1016/S0166-0934\(98\)00174-8](https://doi.org/10.1016/S0166-0934(98)00174-8)
  93. Macatonia SE, Hosken NA, Litton M, Vieira P, Hsieh CS, Culpepper JA, Wysocka M, Trinchieri G, Murphy KM and O'Garra A (1995) Dendritic cells produce IL-12 and direct the development of Th1 cells from naive CD4<sup>+</sup> T cells. *The Journal of Immunology* 154:5071-5079.
  94. Szabo SJ, Kim ST, Costa GL, Zhang X, Fathman CG and Glimcher LH (2000) A Novel Transcription Factor, T-bet, Directs Th1 Lineage Commitment. *Cell* 100:655-669. doi: [https://doi.org/10.1016/S0092-8674\(00\)80702-3](https://doi.org/10.1016/S0092-8674(00)80702-3)
  95. Schroder K, Hertzog PJ, Ravasi T and Hume DA (2004) Interferon- $\gamma$ : an overview of signals, mechanisms and functions. *Journal of Leukocyte Biology* 75:163-189. doi: <https://doi.org/10.1189/jlb.0603252>
  96. Pipkin ME, Sacks JA, Cruz-Guilloty F, Lichtenheld MG, Bevan MJ and Rao A (2010) Interleukin-2 and inflammation induce distinct transcriptional programs that promote the differentiation of effector cytolytic T cells. *Immunity* 32:79-90. doi: 10.1016/j.immuni.2009.11.012
  97. Barry M and Bleackley RC (2002) Cytotoxic T lymphocytes: all roads lead to death. *Nature Reviews Immunology* 2:401-409. doi: 10.1038/nri819
  98. Effros RB, Doherty PC, Gerhard W and Bennink J (1977) Generation of both cross-reactive and virus-specific T-cell populations after immunization with serologically distinct influenza A viruses. *The Journal of experimental medicine* 145:557-568. doi: 10.1084/jem.145.3.557
  99. Grant EJ, Quiñones-Parra SM, Clemens EB and Kedzierska K (2016) Human influenza viruses and CD8<sup>+</sup> T cell responses. *Current Opinion in Virology* 16:132-142. doi: <https://doi.org/10.1016/j.coviro.2016.01.016>
  100. McMichael AJ, Dongworth DW, Gotch FM, Clark A and Potter CW (1983) DECLINING T-CELL IMMUNITY TO INFLUENZA, 1977-82. *The Lancet* 322:762-764. doi: [https://doi.org/10.1016/S0140-6736\(83\)92297-3](https://doi.org/10.1016/S0140-6736(83)92297-3)

101. Zhou J, Matsuoka M, Cantor H, Homer R and Enelow RI (2008) Cutting Edge: Engagement of NKG2A on CD8<sup>+</sup> Effector T Cells Limits Immunopathology in Influenza Pneumonia. *The Journal of Immunology* 180:25-29. doi: 10.4049/jimmunol.180.1.25
102. Damjanovic D, Small CL, Jeyanathan M, McCormick S and Xing Z (2012) Immunopathology in influenza virus infection: uncoupling the friend from foe. *Clin Immunol* 144:57-69. doi: 10.1016/j.clim.2012.05.005
103. Bouvier NM and Lowen AC (2010) Animal Models for Influenza Virus Pathogenesis and Transmission. *Viruses* 2:1530-1563. doi: 10.3390/v20801530
104. Pica N, Iyer A, Ramos I, Bouvier NM, Fernandez-Sesma A, García-Sastre A, Lowen AC, Palese P and Steel J (2011) The DBA.2 mouse is susceptible to disease following infection with a broad, but limited, range of influenza A and B viruses. *Journal of virology* 85:12825-12829. doi: 10.1128/JVI.05930-11
105. Srivastava B, Blazejewska P, Hessmann M, Bruder D, Geffers R, Mael S, Gruber AD and Schughart K (2009) Host genetic background strongly influences the response to influenza A virus infections. *PloS one* 4:e4857-e4857. doi: 10.1371/journal.pone.0004857
106. Kim EH, Park SJ, Kwon HI, Kim SM, Kim YI, Song MS, Choi EJ, Pascua PN and Choi YK (2015) Mouse adaptation of influenza B virus increases replication in the upper respiratory tract and results in droplet transmissibility in ferrets. *Sci Rep* 5:15940. doi: 10.1038/srep15940
107. Prokopyeva E, Kurskaya O, Sobolev I, Solomatina M, Murashkina T, Suvorova A, Alekseev A, Danilenko D, Komissarov A, Fadeev A, Ramsay E, Shestopalov A, Dygai A and Sharshov K (2020) Experimental Infection Using Mouse-Adapted Influenza B Virus in a Mouse Model. *Viruses* 12. doi: 10.3390/v12040470
108. McCullers JA, Hoffmann E, Huber VC and Nickerson AD (2005) A single amino acid change in the C-terminal domain of the matrix protein M1 of influenza B virus confers mouse adaptation and virulence. *Virology* 336:318-26. doi: 10.1016/j.virol.2005.03.028
109. Noymer A and Garenne M (2000) The 1918 influenza epidemic's effects on sex differentials in mortality in the United States. *Population and development review* 26:565-581. doi: 10.1111/j.1728-4457.2000.00565.x
110. Eshima N, Tokumaru O, Hara S, Bacal K, Korematsu S, Tabata M, Karukaya S, Yasui Y, Okabe N and Matsuishi T (2011) Sex- and age-related differences in morbidity rates of 2009 pandemic influenza A H1N1 virus of swine origin in Japan. *PloS one* 6:e19409-e19409. doi: 10.1371/journal.pone.0019409
111. Gavin K, Owen R and Barr IG (2017) Annual report of the National Influenza Surveillance Scheme, 2010. *Commun Dis Intell Q Rep* 41:E348-e368.
112. Wang X-L, Yang L, Chan K-H, Chan K-P, Cao P-H, Lau EH-Y, Peiris JSM and Wong C-M (2015) Age and Sex Differences in Rates of Influenza-Associated Hospitalizations in Hong Kong. *American Journal of Epidemiology* 182:335-344. doi: 10.1093/aje/kwv068
113. Worobey M, Han GZ and Rambaut A (2014) Genesis and pathogenesis of the 1918 pandemic H1N1 influenza A virus. *Proc Natl Acad Sci U S A* 111:8107-12. doi: 10.1073/pnas.1324197111
114. Vermillion MS, Ursin RL, Kuok DIT, Vom Steeg LG, Wohlgemuth N, Hall OJ, Fink AL, Sasse E, Nelson A, Ndeh R, McGrath-Morrow S, Mitzner W, Chan MCW, Pekosz A and Klein SL (2018) Production of amphiregulin and recovery from influenza is greater in males than females. *Biol Sex Differ* 9:24. doi: 10.1186/s13293-018-0184-8

115. Robinson DP, Lorenzo ME, Jian W and Klein SL (2011) Elevated 17beta-estradiol protects females from influenza A virus pathogenesis by suppressing inflammatory responses. *PLoS Pathog* 7:e1002149. doi: 10.1371/journal.ppat.1002149
116. Lorenzo ME, Hodgson A, Robinson DP, Kaplan JB, Pekosz A and Klein SL (2011) Antibody responses and cross protection against lethal influenza A viruses differ between the sexes in C57BL/6 mice. *Vaccine* 29:9246-55. doi: 10.1016/j.vaccine.2011.09.110
117. Vom Steeg LG, Attreed SE, Zirkin B and Klein SL (2019) Testosterone treatment of aged male mice improves some but not all aspects of age-associated increases in influenza severity. *Cell Immunol* 345:103988. doi: 10.1016/j.cellimm.2019.103988
118. Hall OJ, Limjunyawong N, Vermillion MS, Robinson DP, Wohlgemuth N, Pekosz A, Mitzner W and Klein SL (2016) Progesterone-Based Therapy Protects Against Influenza by Promoting Lung Repair and Recovery in Females. *PLoS Pathog* 12:e1005840. doi: 10.1371/journal.ppat.1005840
119. Vermillion MS, Ursin RL, Attreed SE and Klein SL (2018) Estriol Reduces Pulmonary Immune Cell Recruitment and Inflammation to Protect Female Mice From Severe Influenza. *Endocrinology* 159:3306-3320. doi: 10.1210/en.2018-00486
120. Potluri T, Fink AL, Sylvia KE, Dhakal S, Vermillion MS, Vom Steeg L, Deshpande S, Narasimhan H and Klein SL (2019) Age-associated changes in the impact of sex steroids on influenza vaccine responses in males and females. *NPJ Vaccines* 4:29. doi: 10.1038/s41541-019-0124-6
121. Mosnier A, Caini S, Daviaud I, Nauleau E, Bui TT, Debost E, Bedouret B, Agius G, van der Werf S, Lina B, Cohen JM and network G (2015) Clinical Characteristics Are Similar across Type A and B Influenza Virus Infections. *PLoS One* 10:e0136186. doi: 10.1371/journal.pone.0136186
122. Zhong PP, Zhang HL, Chen XF, Liang YF, Lin L, Yang SY, Sheng JY and Li CC (2016) [Lower respiratory tract infection caused by influenza virus A and influenza virus B in Wenzhou, China: a clinical analysis of 366 children]. *Zhongguo Dang Dai Er Ke Za Zhi* 18:117-22. doi: 10.7499/j.issn.1008-8830.2016.02.005
123. Han SB, Rhim J-W, Kang JH and Lee K-Y (2021) Clinical features and outcomes of influenza by virus type/subtype/lineage in pediatric patients. *Translational pediatrics* 10:54-63. doi: 10.21037/tp-20-196
124. Gutiérrez-Pizarra A, Pérez-Romero P, Alvarez R, Aydillo TA, Osorio-Gómez G, Milara-Ibáñez C, Sánchez M, Pachón J and Cordero E (2012) Unexpected severity of cases of influenza B infection in patients that required hospitalization during the first postpandemic wave. *Journal of Infection* 65:423-430. doi: 10.1016/j.jinf.2012.07.004
125. Kim JC, Kim HM, Kang YM, Ku KB, Park EH, Yum J, Kim JA, Kang YK, Lee JS, Kim HS and Seo SH (2014) Severe pathogenesis of influenza B virus in pregnant mice. *Virology* 448:74-81. doi: 10.1016/j.virol.2013.10.001
126. vom Steeg LG and Klein SL (2016) Sex Matters in Infectious Disease Pathogenesis. *PLoS Pathog* 12:e1005374. doi: 10.1371/journal.ppat.1005374
127. Klein SL (2000) The effects of hormones on sex differences in infection: from genes to behavior. *Neuroscience & Biobehavioral Reviews* 24:627-638. doi: [https://doi.org/10.1016/S0149-7634\(00\)00027-0](https://doi.org/10.1016/S0149-7634(00)00027-0)
128. Klein SL, Pekosz A, Passaretti C, Anker M and P O (2010) Sex, gender and influenza. . Geneva: World Health Organization.:pp 1–58.

129. Hoffmann J, Otte A, Thiele S, Lotter H, Shu Y and Gabriel G (2015) Sex differences in H7N9 influenza A virus pathogenesis. *Vaccine* 33:6949-54. doi: 10.1016/j.vaccine.2015.08.044
130. Dinarello CA (1992) Role of Interleukin-1 in Infectious Diseases. *Immunological Reviews* 127:119-146. doi: <https://doi.org/10.1111/j.1600-065X.1992.tb01411.x>
131. Essayan DM, Fox CC, Levi-Schaffer F, Alam R and Rosenwasser LJ (1998) Biologic activities of IL-1 and its role in human disease. *Journal of Allergy and Clinical Immunology* 102:344-350. doi: 10.1016/S0091-6749(98)70118-6
132. Monteiro JM, Harvey C and Trinchieri G (1998) Role of Interleukin-12 in Primary Influenza Virus Infection. *Journal of Virology* 72:4825. doi: 10.1128/JVI.72.6.4825-4831.1998
133. Larcombe AN, Foong RE, Bozanich EM, Berry LJ, Garratt LW, Gualano RC, Jones JE, Dousha LF, Zosky GR and Sly PD (2011) Sexual dimorphism in lung function responses to acute influenza A infection. *Influenza Other Respir Viruses* 5:334-42. doi: 10.1111/j.1750-2659.2011.00236.x
134. Dinarello CA, Bernheim HA, Duff GW, Le HV, Nagabhushan TL, Hamilton NC and Coceani F (1984) Mechanisms of fever induced by recombinant human interferon. *J Clin Invest* 74:906-13. doi: 10.1172/jci111508
135. Akira S and Kishimoto T (1992) IL-6 and NF-IL6 in acute-phase response and viral infection. *Immunol Rev* 127:25-50. doi: 10.1111/j.1600-065x.1992.tb01407.x
136. Chomarat P, Banchereau J, Davoust J and Karolina Palucka A (2000) IL-6 switches the differentiation of monocytes from dendritic cells to macrophages. *Nature Immunology* 1:510-514. doi: 10.1038/82763
137. Yang R, Masters AR, Fortner KA, Champagne DP, Yanguas-Casás N, Silberger DJ, Weaver CT, Haynes L and Rincon M (2016) IL-6 promotes the differentiation of a subset of naive CD8+ T cells into IL-21-producing B helper CD8+ T cells. *Journal of Experimental Medicine* 213:2281-2291. doi: 10.1084/jem.20160417
138. Kozak W, Zheng H, Conn CA, Soszynski D, Ploeg LHvd and Kluger MJ (1995) Thermal and behavioral effects of lipopolysaccharide and influenza in interleukin-1 beta-deficient mice. *American Journal of Physiology-Regulatory, Integrative and Comparative Physiology* 269:R969-R977. doi: 10.1152/ajpregu.1995.269.5.R969
139. García-Sastre A, Durbin RK, Zheng H, Palese P, Gertner R, Levy DE and Durbin JE (1998) The Role of Interferon in Influenza Virus Tissue Tropism. *Journal of Virology* 72:8550. doi: 10.1128/JVI.72.11.8550-8558.1998
140. Flanagan KL, Fink AL, Plebanski M and Klein SL (2017) Sex and Gender Differences in the Outcomes of Vaccination over the Life Course. *Annual Review of Cell and Developmental Biology* 33:577-599. doi: 10.1146/annurev-cellbio-100616-060718
141. Engler RJM, Nelson MR, Klote MM, VanRaden MJ, Huang C-Y, Cox NJ, Klimov A, Keitel WA, Nichol KL, Carr WW, Treanor JJ and Walter Reed Health Care System Influenza Vaccine C (2008) Half- vs Full-Dose Trivalent Inactivated Influenza Vaccine (2004-2005): Age, Dose, and Sex Effects on Immune Responses. *Archives of Internal Medicine* 168:2405-2414. doi: 10.1001/archinternmed.2008.513
142. Hui SL, Chu LW, Peiris JSM, Chan KH, Chu D and Tsui W (2006) Immune response to influenza vaccination in community-dwelling Chinese elderly persons. *Vaccine* 24:5371-5380. doi: <https://doi.org/10.1016/j.vaccine.2006.04.032>
143. Couch RB, Winokur P, Brady R, Belshe R, Chen WH, Cate TR, Sigurdardottir B, Hoepfer A, Graham IL, Edelman R, He F, Nino D, Capellan J and Ruben FL (2007) Safety and

immunogenicity of a high dosage trivalent influenza vaccine among elderly subjects. *Vaccine* 25:7656-7663. doi: <https://doi.org/10.1016/j.vaccine.2007.08.042>  
144. Fan H, Dong G, Zhao G, Liu F, Yao G, Zhu Y and Hou Y (2014) Gender differences of B cell signature in healthy subjects underlie disparities in incidence and course of SLE related to estrogen. *Journal of immunology research* 2014:814598-814598. doi: 10.1155/2014/814598

## Supplemental Tables

**Supplemental Table 1.** Raw cytokine concentrations in spleens.

dpi	3												7											
Sex	Male												Male											
ID	1	2	3	4	5	6	7	8	9	10	11	12	24	25	26	27	28	29	30	31	32	33		
BAFF	615.6	31.85	352	31.85	2462.5	126.47	4791.49	4791.49	6715.31	957.81	2462.5	2462.5	14775	126.47	2462.5	2462.5	14775	6715.31	9850	4791.49	14775	2462.5		
G-CSF	18.65	95.67	95.67	47	92.41	92.41	92.41	47	92.41	108.99	92.41	47	47	47	47	47	92.41	92.41	92.41	47	92.41	1737.5		
GM-CSF	158.1	576.1	576.1	183.6	927.2	268.5	268.5	3055.4	135.0	702.2	268.5	927.2	135.0	268.5	135.0	135.0	3055.4	135.0	1862.7	927.2	927.2	927.2		
IFN-α	1017.3	695.1	287.4	1027.6	920.0	3406.2	1838.6	920.3	1838.6	2641.5	920.0	920.0	2641.5	4155.4	920.0	920.0	920.0	1838.6	3406.2	920.3	9463.1	1838.6		
IFN-γ	38.4	46.0	455.6	265.1	264.2	1296.3	1296.3	264.2	1945.0	24.6	104.0	1945.0	239.8	264.2	296.9	1945.0	1296.3	104.0	264.2	1296.3	296.9	239.8		
IL-1α	722.0	575.1	753.2	319.0	1677.2	837.0	1204.7	1204.7	1677.2	1093.5	837.0	1204.7	7435.2	3265.4	837.0	3265.4	3265.4	3265.4	1677.2	837.0	3265.4	837.0		
IL-1β	237.3	22.0	188.0	22.0	113.0	113.0	224.7	224.7	224.7	27.0	681.8	113.0	432.7	113.0	224.7	113.0	113.0	113.0	113.0	113.0	224.7	113.0		
IL-2	41.2	91.9	94.0	187.5	225.4	225.4	113.0	1661.6	225.4	103.4	852.4	113.0	510.9	225.4	225.4	225.4	113.0	23.9	1661.6	113.0	113.0	113.0		
IL-2R	62.66	75.89	38	38	11.56	11.56	39.92	26.35	39.92	101.63	11.56	67.99	11.56	39.92	11.56	99.04	67.99	561.92	39.92	11.56	39.92	39.92		
IL-3	24.15	20.52	236.07	20.52	46.6	2.43	115.58	115.58	115.58	88.01	115.58	77.96	46.6	21.39	46.6	46.6	46.6	77.96	46.6	46.6	115.58	210.7		
IL-4	43	264	133	133	1090	1090	1090	1090	1090	160	1090	1090	545	1090	545	3606	1090	545	1090	545	1090	1090		
IL-5	237	22	22	43.28	23	44.56	800.98	44.56	44.56	44.56	1611.62	415.62	800.98	800.98	23	415.62	44.56	1200.23	44.56	44.56	44.56	44.56		
IL-6	1110	2548	112	112	288	5800	4279	5800	5800	1110	5800	5800	288	4279	4279	288	288	5800	4279	4279	5800			
IL-7	2908	1185	3656	1185	255	5125	5125	5125	6922	247	20500	3556	5125	6922	6922	6922	3556	255	9328	6922	9328	5125		
IL-7Rα	342	751	2597	751	3750	4203	19950	19950	3325	683	19950	19950	19950	19950	716	4203	4748	6828	3325	19950	19950	3325		
IL-10	786	531	266	531	2152	7681	7681	6544	2152	2360	2152	2152	27952	9575	2152	10522	6544	7681	6544	1077	11530			
IL-12p70	16	136.7	16	30.22	60	629.09	60	60	119.39	23	60	629.09	119.39	119.39	60	629.09	629.09	136.7	119.39	119.39	60	629.09		
IL-13	66.81	131.31	131.31	131.31	124	246.95	713.73	124	464.08	311.74	124	124	989.92	124	124	124	124	464.08	713.73	74.13	246.95	124		
IL-15/IL-15R	252.85	200.69	200.69	101	148.4	253.94	253.94	253.94	148.4	252.85	148.4	253.94	148.4	148.4	148.4	148.4	148.4	253.94	148.4	148.4	75	266.41		
IL-17A	294	575	2917	575	478	4700	126	126	741	209	1174	126	1174	294	294	64	126	478	478	64	7050			
IL-18	130	306	1375	306	130	52226	130	14206	3506	130	5416	3506	14206	913	5416	5416	10705	5416	913	2018	5416	7797		
IL-19	14568	9087	9087	9087	35928	13353	8521	26706	35928	8263	26706	42933	35928	13353	26706	42933	35928	26706	26706	26706	13353	58476		
IL-22	263	377	377	377	207	207	414	414	414	207	414	207	2018	207	58	13433	58	207	414	414	414	207		
IL-23	2435	298	298	5346	572	4874	6033	2841	2841	323	7295	3812	3812	10152	6033	8666	6033	10152	4874	2841	4874	4874		
IL-25	413	101	406	101	180	982	982	180	359	413	56	359	982	359	180	3535	1297	2251	982	669	359	982		
IL-27	133	56	448	56	1854	135	351	698	351	133	135	1194	56	698	56	9984	698	56	698	135	135	698		
IL-28	12634	1202	21752	4575	54025	216100	216100	216100	71043	5787	71043	172439	71043	2738	89993	71043	54025	89993	138889	138889	2738	216100		
IL-31	10504	3680	3680	4181	2666	7144	7144	2666	10650	3790	2666	7144	5195	5195	2666	14048	10650	8929	7144	7144	10650			
IL-33	11125	43999	11681	5841	9755	44500	32412	55530	44500	13114	55530	40542	44500	36747	44500	55530	36747	66733	49171	36747	9755	267000		
IL-33R	134	3557	279	279	3063	6125	27126	27126	3063	1732	3063	5050	40690	3063	27126	40690	6125	27126	6125	5050	27126	27126		
LIF	21.94	206.9	131.37	131.37	102.66	102.66	52	249.68	168.52	11	49.03	102.66	49.03	102.66	102.66	52	102.66	52	102.66	52	102.66	102.66		
M-CSF	21.22	1.95	13.39	1.95	31.59	91.48	148	31.59	91.48	21.22	91.48	148	308.84	91.48	91.48	801.34	91.48	308.84	91.48	91.48	46	46		
RANKL	130.5	54.7	70.9	54.7	127.6	279.0	2235.1	503.6	279.0	97.6	381.0	822.8	1026.1	503.6	127.6	822.8	279.0	503.6	1263.9	1026.1	195.3	279.0		
TNFα	649.97	99	99	99	166.73	166.73	84	84	84	493.5	166.73	84	493.5	166.73	166.73	166.73	166.73	166.73	321.14	166.73	166.73	166.73		
CXCL5	763	3092	282	282	10005	2756	2756	1378	11154	148	2756	10005	73200	2756	8581	73200	10005	18614	14210	15233	12200	11154		
CCL11	1082	4275	2850	4275	4275	2850	4275	4275	2850	4275	2850	713	941	2850	2850	4275	713	4275	941	4275	713	2850		
CXCL1	1119	64	64	126	577	212	212	577	1100	98	212	302	212	143	143	143	143	143	302	143	143	302		
CXCL10	605	6	6	4	1710	1710	1710	1710	1710	427	1710	1710	1138	1710	1710	1138	1710	1710	1710	1710	1710	1138		
CCL2	1045	104	536	268	288	288	574	2088	3529	1918	288	288	574	574	574	288	574	3529	288	574	288	574		
CCL7	1646	737	31	31	825	825	647	1049	1859	821	647	647	1859	647	825	4950	1440	4950	825	1049	1440	4950		
CCL3	46.71	53.28	45.85	38.52	277.79	132.92	154.13	93.75	154.13	107.86	93.75	132.92	75.72	176.47	176.47	433.97	306.28	224.67	224.67	93.75	545.3	132.92		
CCL4	37.49	67.19	67.19	67.19	14.91	14.91	14.91	8	110.78	64.55	30.94	14.91	14.91	14.91	30.94	313.81	14.91	195.6	52.04	4.02	14.91	30.94		
CXCL2	18.29	43.24	22	22	73.87	73.87	73.87	73.87	73.87	49.47	206.92	73.87	143.32	73.87	73.87	887.18	143.32	380.99	206.92	206.92	206.92	73.87		
CCL5	797.9	308.1	171.7	202.3	414.7	436.2	669.6	1298.4	639.7	1122.9	801.7	700.8	1243.0	801.7	838.1	7154.4	956.6	1090.6	838.1	956.6	583.1	1416.8		
Betacellulin	243.21	60	367.73	367.73	71	140.65	71	403.86	979.77	452.46	300.63	537.04	140.65	140.65	71	140.65	71	537.04	37.98	300.63	37.98	140.65		
Leptin	1203	13031	13031	13031	6661	3331	6661	3331	3331	1508	35157	3331	3331	20462	3331	14797	3331	20462	3331	6661	3331	14797		
VEGF-A	9.7	427.9	427.9	427.9	1520.1	1520.1	1520.1	6349.8	761.0	124.0	1520.1	1520.1	6349.8	1520.1	1520.1	5841.0	1520.1	5841.0	1520.1	6349.8	761.0	1520.1		

Continued Supplemental Table 1

dpi	3											7										
Sex	Female											Female										
ID	13	14	15	16	17	18	19	20	21	22	23	34	35	36	37	38	39	40	41	42	43	
BAFF	823.55	174.2	352	2462.5	14775	4791.49	2462.5	2462.5	4791.49	2462.5	4791.49	4791.49	4791.49	14775	9850	14775	64	14775	14775	3465.95	4791.49	
G-CSF	10	95.67	95.67	2940.64	92.41	47	92.41	92.41	92.41	92.41	47	92.41	92.41	92.41	92.41	1059.94	47	47	92.41	92.41	47	
GM-CSF	702.2	183.6	684.7	927.2	927.2	135.0	135.0	927.2	135.0	135.0	927.2	927.2	135.0	135.0	927.2	927.2	135.0	135.0	927.2	135.0	135.0	
IFN- $\alpha$	1017.3	144.0	1343.2	1838.6	920.0	1838.6	1838.6	920.3	1838.6	1838.6	1838.6	3406.2	1838.6	1838.6	1838.6	7909.2	1838.6	3406.2	920.0	7146.6	4155.4	
IFN- $\gamma$	11.4	46.0	670.2	1296.3	1296.3	264.2	296.9	1296.3	264.2	1296.3	1945.0	1945.0	264.2	1945.0	1296.3	1296.3	264.2	104.0	104.0	264.2	104.0	
IL-1 $\alpha$	319.0	676.6	753.2	19989.0	19989.0	138.5	837.0	1677.2	837.0	837.0	3265.4	837.0	837.0	1677.2	1677.2	7435.2	1677.2	19989.0	19989.0	1677.2	837.0	
IL-1 $\beta$	22.0	188.0	22.0	113.0	113.0	113.0	113.0	224.7	224.7	113.0	68.5	224.7	224.7	113.0	224.7	113.0	113.0	113.0	113.0	113.0	113.0	
IL-2	41.2	386.5	187.5	225.4	113.0	510.9	225.4	225.4	225.4	225.4	225.4	225.4	225.4	225.4	225.4	23.9	852.4	23.9	852.4	510.9	225.4	
IL-2R	62.66	38	38	11.56	53.67	11.56	11.56	39.92	11.56	11.56	6	11.56	11.56	83.07	39.92	11.56	26.35	6	11.56	6	11.56	
IL-3	88.01	20.52	336.62	46.6	46.6	46.6	115.58	46.6	46.6	2.43	46.6	2.43	2.43	159.72	46.6	46.6	115.58	2.43	210.7	2.43	46.6	
IL-4	160	57	264	1090	545	1090	1090	1090	1090	1090	3606	1090	545	545	1090	3606	1090	1090	1090	1090	545	
IL-5	237	43.28	476.72	1611.62	800.98	1200.23	800.98	44.56	800.98	44.56	23	44.56	44.56	415.62	800.98	23	44.56	44.56	800.98	1611.62	44.56	
IL-6	1110	112	2548	5800	4279	288	4279	3320	5800	4279	288	4279	4279	288	4279	288	5800	288	6499	5800	5072	
IL-7	2908	5126	4444	20500	6922	9328	3556	5125	5125	5125	20500	6922	5125	255	255	255	255	5125	5125	255	255	
IL-7R $\alpha$	342	376	4001	3750	2854	4203	716	19950	19950	2854	3325	13300	716	5501	5501	19950	716	5501	5501	19950	19950	
IL-10	1571	266	266	8647	7681	7681	2152	7681	2152	6544	7681	2152	2152	2152	10522	2152	2152	11530	8647	6544	2152	
IL-12p70	23	157.67	120.67	629.09	945	119.39	60	60	102.41	629.09	629.09	119.39	60	629.09	945	945	119.39	102.41	629.09	60	102.41	
IL-13	21.46	131.31	30.7	124	124	124	124	124	124	124	124	124	124	1288.91	246.95	124	124	124	124	124	246.95	
IL-15/IL-15R	101	200.69	101	253.94	253.94	148.4	148.4	148.4	253.94	148.4	278.1	148.4	148.4	148.4	253.94	75	148.4	148.4	75	148.4	148.4	
IL-17A	147	575	575	64	1174	126	478	478	478	478	126	126	478	64	1174	1174	478	741	64	64	478	
IL-18	130	153	1375	18368	29008	18368	2018	29008	3506	5416	10705	23273	2018	29008	35671	23273	5416	7797	14206	2018	2018	
IL-19	8263	9087	9087	42933	48780	26706	26706	35928	26706	26706	35928	13353	26706	13353	48780	35928	26706	8521	26706	26706	26706	
IL-22	525	377	1013	207	207	414	207	2018	414	1121	414	207	207	207	414	58	207	207	5539	414	1121	
IL-23	298	298	596	7295	8666	7295	4874	7295	2841	10152	2841	3812	1144	3812	4874	1144	4874	4874	1955	2841	2841	
IL-25	413	406	101	1614	359	359	982	359	982	982	359	669	359	180	180	669	359	1614	982	982	982	
IL-27	133	110	110	698	6404	698	56	698	56	351	351	27	135	1194	56	135	135	6404	698	135	27	
IL-28	11573	21752	21752	324150	324150	71043	216100	216100	216100	216100	216100	54025	54025	2738	2738	54025	54025	89993	2738	37340	54025	
IL-31	3790	3680	2338	7144	1334	2666	2666	2666	2666	2666	7144	7144	2666	7144	7144	10650	2666	5195	14048	7144	2666	
IL-33	3503	11681	24685	55530	55530	32412	36747	36747	36747	44500	55530	44500	9755	44500	40542	44500	36747	9755	36747	36747	44500	
IL-33R	1732	279	279	27126	6125	3063	3063	3063	6125	6125	27126	27126	6125	6125	6125	6125	6125	40690	27126	6125	3063	
LIF	105.66	131.37	131.37	52	52	52	102.66	249.68	49.03	52	52	52	52	249.68	52	52	102.66	52	102.66	52	102.66	
M-CSF	21.22	13.39	13.39	202.74	202.74	91.48	91.48	46	202.74	46	46	91.48	46	46	46	46	91.48	31.59	308.84	46	46	
RANKL	212.4	28.6	28.6	503.6	381.0	279.0	503.6	649.8	279.0	127.6	1263.9	127.6	279.0	381.0	503.6	33.5	381.0	279.0	195.3	33.5	127.6	
TNF $\alpha$	649.97	197.37	400.69	493.5	701.85	84	166.73	166.73	166.73	321.14	493.5	166.73	166.73	166.73	166.73	84	166.73	166.73	166.73	166.73	166.73	
CXCL5	1635	2187	3092	48800	73200	10005	2756	8581	2756	2756	18614	14210	10005	21345	14210	73200	16295	73200	13207	11154	16295	
CCL11	938	2850	713	2850	80	713	4275	2850	4275	713	4275	4275	158	941	4275	4275	713	2850	4275	713	713	
CXCL1	72	64	356	302	212	577	143	39	419	302	302	143	143	143	143	143	302	143	143	143	87	
CXCL10	1053	6	6	1710	1710	263	1710	1710	1138	1710	1710	1710	1138	1710	1710	1710	1138	1710	1710	1710	61	
CCL2	523	268	268	288	288	288	288	288	288	288	288	288	288	288	574	574	288	288	288	288	288	
CCL7	253	31	16	4950	4950	825	191	647	1049	96	1049	1049	647	1049	3300	4950	551	3300	1049	647	825	
CCL3	56.28	23.68	53.28	176.47	93.75	58.66	93.75	93.75	132.92	93.75	176.47	75.72	93.75	250.6	336.1	277.79	75.72	585.61	399.91	93.75	132.92	
CCL4	64.55	100.68	67.19	52.04	14.91	52.04	52.04	52.04	14.91	8	14.91	8	14.91	52.04	52.04	52.04	8	8	52.04	8	14.91	
CXCL2	18.29	22	43.24	435.57	488.94	73.87	73.87	73.87	73.87	206.92	206.92	73.87	206.92	267.13	73.87	488.94	73.87	643.36	324.97	206.92	206.92	
CCL5	1715.6	308.1	233.5	373.7	5088.6	669.6	610.8	1090.6	481.7	801.7	733.1	669.6	458.5	1243.0	414.7	1416.8	583.1	1090.6	373.7	414.7	610.8	
Betacellulin	243.21	60	367.73	367.73	1389.62	300.63	140.65	71	71	403.86	140.65	71	140.65	37.98	140.65	71	140.65	71	300.63	216.07	300.63	
Leptin	14542	13031	13031	26861	3331	3331	3331	6661	3331	3331	35157	26861	3331	20462	35157	35157	3331	6661	20462	3331	6661	
VEGF-A	9.7	427.9	214.0	6950.0	1520.1	1520.1	1520.1	1520.1	1520.1	1520.1	1520.1	1520.1	1520.1	5841.0	1520.1	1520.1	1520.1	5841.0	6349.8	1520.1	1520.1	



Continued Supplemental Table 1

dpi	Mock																	
Sex	Male									Female								
ID	44	45	46	47	48	49	50	51	52	53	54	55	56	57	58	59	60	61
<b>BAFF</b>	615.6	615.6	615.6	767.52	812.89	748.28	748.28	748.28	748.28	715.55	665.63	715.55	615.6	532.14	880.96	748.28	615.6	615.6
<b>G-CSF</b>	10	10	18.65	18.65	97.67	97.67	97.67	97.67	97.67	18.65	10	18.65	10	97.67	97.67	49	97.67	49
<b>GM-CSF</b>	3.0	331.2	4.6	331.2	947.4	310.0	618.4	1922.3	618.4	4.6	331.2	4.6	331.2	618.4	1274.0	947.4	618.4	618.4
<b>IFN-<math>\alpha</math></b>	33.0	1017.3	33.0	1017.3	1661.8	1661.8	74.0	1661.8	1047.5	1017.3	33.0	1017.3	1017.3	1661.8	1661.8	146.1	1047.5	146.1
<b>IFN-<math>\gamma</math></b>	6.0	6.0	6.0	38.4	34.0	67.9	67.9	34.0	67.9	11.4	38.4	11.4	11.4	67.9	34.0	67.9	34.0	67.9
<b>IL-1<math>\alpha</math></b>	319.0	319.0	319.0	319.0	638.5	319.0	319.0	319.0	638.5	1411.8	1411.8	1093.5	319.0	638.5	319.0	319.0	319.0	319.0
<b>IL-1<math>\beta</math></b>	53.9	27.0	237.3	237.3	397.9	397.9	78.3	397.9	397.9	53.9	53.9	237.3	237.3	397.9	397.9	397.9	78.3	78.3
<b>IL-2</b>	174.8	174.8	41.2	174.8	338.8	102.7	52.0	52.0	338.8	174.8	174.8	103.4	41.2	102.7	102.7	52.0	216.8	102.7
<b>IL-2R</b>	32	62.66	62.66	62.66	124.02	124.02	63	124.02	124.02	62.66	32	62.66	32	124.02	124.02	63	124.02	63
<b>IL-3</b>	24.15	24.15	88.01	24.15	189.14	10.62	110.44	110.44	110.44	24.15	88.01	24.15	24.15	10.62	110.44	10.62	67.86	110.44
<b>IL-4</b>	43	43	43	160	289	289	289	289	145	43	43	160	84	289	145	289	289	289
<b>IL-5</b>	237	237	237	473.2	283	565.84	283	565.84	283	237	728.11	237	237	565.84	565.84	283	283	283
<b>IL-6</b>	556	1110	556	2001	3912	3912	3582	3186	3582	1110	2001	1110	556	3186	3582	3186	3186	284
<b>IL-7</b>	124	247	247	2313	1162	581	581	581	581	247	247	124	2908	581	1162	581	581	1162
<b>IL-7Ra</b>	342	342	342	683	365	365	365	365	728	342	342	683	342	365	365	728	728	365
<b>IL-10</b>	786	786	786	786	528	528	528	528	528	786	786	786	786	528	528	528	528	528
<b>IL-12p70</b>	23	23	23	23	23	23	23	25.88	13	23	23	23	23	25.88	23	23	25.88	25.88
<b>IL-13</b>	21.46	21.46	66.81	112.91	84.28	84.28	3.01	84.28	195.93	21.46	112.91	209.43	11	3.01	195.93	3.01	3.01	3.01
<b>IL-15/IL-15R</b>	252.85	252.85	252.85	252.85	148.12	148.12	148.12	148.12	526.37	252.85	252.85	252.85	127	148.12	148.12	75	148.12	148.12
<b>IL-17A</b>	147	209	147	209	137	137	272	137	272	147	209	147	209	272	272	137	925	137
<b>IL-18</b>	130	130	130	130	279	279	279	556	279	130	130	130	130	279	279	279	279	279
<b>IL-19</b>	4132	4132	4132	4132	15274	15274	3286	15274	15274	8263	4132	8263	4132	15274	26619	3286	15274	26619
<b>IL-22</b>	263	263	227	525	822	822	822	822	822	227	263	525	263	822	822	822	2538	822
<b>IL-23</b>	323	644	323	2435	644	644	644	644	644	644	644	323	323	644	644	323	5211	5211
<b>IL-25</b>	207	207	207	207	501	207	501	207	501	207	207	207	207	207	285	207	207	207
<b>IL-27</b>	67	37	67	133	128	64	128	128	128	67	67	67	67	64	128	64	64	64
<b>IL-28</b>	5787	13506	11573	11573	2966	13506	16256	11746	13506	11573	13506	11573	12634	16256	2966	2966	16256	13506
<b>IL-31</b>	3790	3790	3790	3790	2284	2284	2284	7774	9892	3790	5205	3790	3790	8991	2284	2284	2284	8991
<b>IL-33</b>	5563	5563	5563	9666	44500	44500	9867	9867	9867	5563	5563	5563	9666	44500	9867	9867	44500	4934
<b>IL-33R</b>	67	1732	134	1732	2218	10568	2218	2218	4435	897	1732	134	134	2218	1822	2218	2218	4435
<b>LIF</b>	21.94	21.94	21.94	11	51	51	27.64	100.1	100.1	21.94	21.94	21.94	105.66	27.64	51	51	100.1	51
<b>M-CSF</b>	11	11	21.22	41.85	15	29.6	29.6	15	15	21.22	11	11	11	15	15	15	15	29.6
<b>RANKL</b>	212.4	87.7	61.2	142.6	24.0	24.0	24.0	122.7	24.0	142.6	97.6	12.0	97.6	24.0	24.0	24.0	122.7	24.0
<b>TNF<math>\alpha</math></b>	97	97	193.59	683.37	172.66	172.66	172.66	564.78	172.66	193.59	600.46	193.59	193.59	172.66	172.66	172.66	564.78	172.66
<b>CXCL5</b>	75	763	763	1226	1005	1005	1005	503	1005	763	75	75	763	579	1005	1005	1005	1005
<b>CCL11</b>	4275	713	1285	1285	1015	1015	1015	713	1015	938	1285	938	1285	1015	1015	1015	158	1015
<b>CXCL1</b>	144	536	72	293	205	103	205	205	205	72	144	144	144	205	205	103	205	205
<b>CXCL10</b>	1186	605	605	215	190	190	190	190	567	605	913	427	605	567	1082	190	809	190
<b>CCL2</b>	523	523	523	509	990	1979	1979	990	1979	523	523	523	523	2693	1979	990	1363	1363
<b>CCL7</b>	821	821	253	1154	181	181	181	181	181	821	821	253	600	181	181	181	181	181
<b>CCL3</b>	46.71	56.28	37.45	37.45	320.2	287.62	287.62	287.62	334.35	20.11	20.11	37.45	28.56	287.62	267.78	287.62	347.56	287.62
<b>CCL4</b>	5	8.21	23.66	37.49	158.48	35	130.05	69.45	130.05	64.55	23.66	8.21	8.21	69.45	130.05	130.05	35	69.45
<b>CXCL2</b>	10	18.29	18.29	70.86	38.95	38.95	38.95	38.95	148.77	18.29	10	10	18.29	38.95	38.95	20	38.95	38.95
<b>CCL5</b>	1982.0	1037.8	1167.3	1094.0	1146.8	769.1	664.2	1099.7	690.1	957.4	1037.8	615.0	1094.0	906.9	1115.3	1489.1	1068.9	921.1
<b>Betacellulin</b>	59	117.44	117.44	117.44	247	247	492.35	444.81	247	243.21	243.21	117.44	117.44	444.81	492.35	247	247	247
<b>Leptin</b>	3015	8452	1203	5747	2456	2456	2456	2456	2456	5747	3015	3015	5747	2456	7226	2456	2456	2456
<b>VEGF-A</b>	9.7	9.7	9.7	61.8	390.3	390.3	390.3	390.3	390.3	1178.2	5.0	9.7	9.7	390.3	390.3	390.3	1178.2	390.3

**Supplemental Table 2.** Raw cytokine concentrations in sera.

dpi	3												7											
Sex	Male												Male											
ID	1	2	3	4	5	6	7	8	9	10	11	12	24	25	26	27	28	29	30	31	32	33		
BAFF	148.24	1025.37	1025.37	148.24	22	249	249	1025.37	148.24	41.77	148.24	148.24	41.77	148.24	148.24	148.24	148.24	148.24	22	1025.37	148.24	1025.37		
G-CSF	62	13.05	122.38	122.38	122.38	18.65	10	62	13.05	13.05	13.05	122.38	62	122.38	122.38	122.38	62	62	62	62	62	122.38		
GM-CSF	1667.7	47.31	47.31	47.31	47.31	331.21	4.58	47.31	24	47.31	47.31	47.31	47.31	47.31	47.31	24	47.31	24	47.31	47.31	47.31	47.31		
IFN-alpha	4406.2	4406.2	4406.2	4406.2	4406.2	33	33	4406.2	2204	4406.2	2204	4406.2	4406.2	4406.2	4406.2	5723.7	4406.2	4406.2	2204	5723.7	2204	4406.2		
IFN-gamma	9	319.14	17.07	74.2	9	38.39	38.39	319.14	9	17.07	319.14	17.07	9	9	319.14	319.14	9	17.07	9	9	17.07	319.14		
IL-1 alpha	322	643.14	322	643.14	163.77	721.98	102	322	163.77	322	322	322	322	322	643.14	322	322	322	322	322	322	322		
IL-1 beta	259	516.49	259	516.49	259	53.94	27	259	259	259	259	259	516.49	259	259	259	259	259	259	259	516.49	259		
IL-2R	16.16	16.16	16.16	114.51	192.34	62.66	32	192.34	16.16	192.34	16.16	16.16	16.16	16.16	16.16	9	16.16	16.16	192.34	9	9	9		
IL-5	262	1865.25	522.16	262	262	237	237	522.16	262	262	1865.3	262	262	262	262	262	522.16	262	262	262	262	262		
IL-6	1832	1832	3663.06	1832	1832	556	556	1832	1832	4681.6	1832	1832	4681.6	1832	1832	1832	1832	1832	1832	1832	4681.6	1832		
IL-7	553.0	1104.9	1104.9	1104.9	1104.9	246.5	124.0	1104.9	1104.9	1104.9	1104.9	1104.9	1104.9	1104.9	1104.9	1104.9	1104.9	1104.9	1104.9	1104.9	1104.9	1104.9		
IL-9	286.4	286.4	286.4	286.4	286.4	286.4	286.4	286.4	286.4	286.4	144.0	286.4	144.0	286.4	144.0	286.4	144.0	144.0	286.4	144.0	144.0	144.0		
IL-10	8638.2	8638.2	8638.2	8638.2	8638.2	700.8	786.0	8638.2	8638.2	8638.2	4320.0	8638.2	8638.2	8638.2	8638.2	8638.2	8638.2	8638.2	8638.2	4320.0	4320.0	8638.2		
IL-12p70	2.14	11.23	11.23	2.14	2.14	23	23	11.23	11.23	2.14	11.23	2.14	2.14	11.23	11.23	2.14	23.97	11.23	11.23	11.23	2.14	11.23		
IL-15/IL-15R	951.73	951.73	951.73	951.73	951.73	815.39	127	951.73	951.73	476	951.73	476	951.73	951.73	951.73	951.73	476	951.73	951.73	951.73	951.73	951.73		
IL-17A	143	1155.41	1155.41	143	285.61	293.8	147	143	143	143	143	143	143	143	143	143	1155.41	143	143	143	143	143		
IL-18	1491	8250	2981	2981	2981	279	279	1491	1491	1491	2981	2981	2981	2981	2981	1491	1491	1491	1491	1491	1491	1491		
IL-19	5271	180	5271	2636	5271	4048	4132	13333	2636	5271	2636	2636	5271	2636	2636	2636	2636	2636	23339	5271	2636	23339		
IL-23	1059	1059	1059	1059	530	2672	323	1059	1059	530	1059	530	1059	530	1059	530	1059	1059	1059	1059	530	530		
IL-25	216	216	1317	216	216	413	207	216	216	216	216	216	216	861	216	216	216	216	216	431	216	216		
IL-28	86033	52261	52261	52261	52261	5787	5787	52261	52261	52261	52261	52261	52261	52261	52261	52261	26130	52261	52261	52261	52261	26130		
IL-31	9814	4907	9814	4907	9814	3790	3790	9814	9814	9814	9814	9814	9814	9814	9814	9814	9814	4907	4907	4907	9814	4907		
IL-33	44500	59654	44500	44500	44500	11125	5563	44500	44500	22250	44500	59654	22250	44500	44500	22250	22250	22250	44500	59654	44500	52890		
IL-33R	411.98	411.98	411.98	411.98	411.98	896.96	133.69	12619.57	411.98	411.98	411.98	411.98	411.98	411.98	411.98	411.98	411.98	12619.57	411.98	411.98	411.98	411.98		
M-CSF	156.43	29.39	15	15	15	11	11	15	15	15	15	15	29.39	29.39	15	15	15	15	15	15	29.39	15		
RANKL	20	20	20	20	20	3	3	20	20	20	145.42	86.91	20	4.72	20	145.42	20	86.91	20	20	20	20		
TNF alpha	335.96	335.96	335.96	335.96	168	649.97	97	335.96	335.96	335.96	168	168	168	168	335.96	168	335.96	335.96	168	335.96	168	335.96		
CCL11	629	629	2850	629	629	713	156	629	315	629	629	315	629	2850	2850	629	2850	629	629	629	629	629		
CXCL1	53.13	121	121	241.58	241.58	143.89	143.89	241.58	241.58	442.05	121	121	121	649.12	121	53.13	121	121	121	121	121	121		
CXCL10	1695.6	194	194	194	194	108	108	194	194	194	194	194	194	194	194	1030.44	194	194	194	194	2433.53	194		
CCL2	257.1	257.1	257.1	1736.5	257.1	1045.1	523.0	257.1	257.1	1736.5	257.1	257.1	257.1	257.1	1736.5	257.1	257.1	257.1	257.1	257.1	257.1	257.1		
CCL7	127.0	253.5	253.5	253.5	253.5	127.0	253.5	253.5	253.5	253.5	127.0	127.0	127.0	127.0	253.5	253.5	253.5	253.5	253.5	253.5	253.5	127.0		
CCL4	1.05	115.6	1.05	115.6	115.6	8.21	8.21	54.97	1.05	115.6	243.43	1.05	1.05	1.05	1.05	115.6	115.6	1.05	1.05	1.05	1.05	1.05		
CXCL2	64.19	33	33	64.19	33	10	10	33	33	33	33	33	64.19	64.19	64.19	33	33	33	33	33	64.19	33		
Leptin	54.0	54.0	54.0	54.0	54.0	1508.0	1508.0	54.0	54.0	54.0	15626.8	54.0	54.0	54.0	54.0	54.0	54.0	54.0	54.0	54.0	54.0	54.0		
VEGF-A	1709.1	1709.1	1709.1	1709.1	855.0	124.0	9.7	855.0	855.0	1709.1	855.0	1709.1	1709.1	1709.1	1709.1	1709.1	855.0	1709.1	855.0	1709.1	1709.1	1709.1		

Continued Supplemental Table 2

dpi	3											7										
Sex	Female											Female										
ID	13	14	15	16	17	18	19	20	21	22	23	34	35	36	37	38	39	40	41	42	43	
BAFF	22	148.24	148.24	148.24	148.24	249	22	386.4	148.24	22	22	148.24	148.24	386.4	148.24	148.24	1025.37	148.24	22	41.77	22	
G-CSF	62	122.38	62	122.38	13.05	10	62	122.38	62	62	122.38	62	62	62	62	122.38	62	62	62	62	62	
GM-CSF	47.31	47.31	47.31	47.31	47.31	4.58	47.31	24	47.31	24	47.31	47.31	47.31	47.31	47.31	47.31	47.31	47.31	47.31	24	47.31	
IFN-alpha	4406.2	4406.2	4406.2	4406.2	4406.2	1017.3	2204	2204	4406.2	2204	4406.2	5723.7	2204	4406.2	5723.7	4406.2	2204	4406.2	2204	5723.7	4406.2	
IFN-gamma	17.07	319.14	17.07	17.07	9	11.44	9	9	9	9	17.07	17.07	17.07	17.07	9	74.2	9	74.2	17.07	17.07	17.07	
IL-1 alpha	643.14	643.14	322	322	322	102	2202.66	643.14	643.14	322	322	322	322	643.14	322	322	322	322	322	322	322	
IL-1 beta	259	259	259	259	259	27	259	516.49	259	259	259	259	259	516.49	259	259	259	1083.22	241.35	516.49	516.49	
IL-2R	9	192.34	16.16	16.16	114.51	62.66	192.34	114.51	9	192.34	192.34	9	9	16.16	192.34	16.16	9	16.16	114.51	16.16	16.16	
IL-5	522.16	522.16	262	262	262	237	262	262	522.16	1219.2	262	262	262	262	262	262	262	262	522.16	522.16	522.16	
IL-6	1832	1832	1832	1832	1832	556	1832	1832	1832	1832	3663.1	1832	1832	4681.6	1832	1832	1832	1832	1832	1832	1832	
IL-7	553.0	1104.9	1104.9	1104.9	1104.9	246.5	1104.9	1104.9	1104.9	1104.9	1104.9	1104.9	1104.9	1104.9	1104.9	553.0	1104.9	1104.9	1104.9	1104.9	1104.9	
IL-9	286.4	286.4	286.4	286.4	286.4	144.0	144.0	286.4	286.4	286.4	144.0	286.4	286.4	144.0	286.4	286.4	144.0	286.4	286.4	286.4	286.4	
IL-10	8638.2	8638.2	8638.2	8638.2	8638.2	786.0	8638.2	8638.2	8638.2	8638.2	4320.0	4320.0	8638.2	8638.2	8638.2	8638.2	8638.2	8638.2	4320.0	8638.2		
IL-12p70	11.23	11.23	4.89	11.23	2.14	23	11.23	2.14	4.89	11.23	2.14	2.14	2.14	169.97	2.14	2.14	2.14	48.23	2.14	11.23	11.23	
IL-15/IL-15R	951.73	951.73	951.73	476	951.73	127	951.73	951.73	951.73	476	476	951.73	951.73	951.73	951.73	951.73	476	951.73	951.73	951.73	951.73	
IL-17A	143	1155.41	143	143	143	293.8	143	143	143	143	143	1155.41	1155.41	143	143	285.61	1155.41	285.61	143	143		
IL-18	2981	1491	2981	2981	53626	279	2981	2981	2981	1491	1491	1491	2981	2981	1491	1491	1491	2981	1491	1491	1491	
IL-19	23339	23339	5271	2636	5271	4132	23339	2636	23339	180	23339	5271	23339	13333	2636	23339	5271	23339	5271	2636	2636	
IL-23	530	1059	530	1059	530	323	1059	530	1059	530	530	530	530	1059	530	530	530	4923	530	530	1059	
IL-25	216	216	431	216	216	207	216	431	216	216	216	1317	216	216	216	216	216	216	216	216	216	
IL-28	107674	86033	26130	52261	52261	5787	52261	26130	52261	52261	52261	52261	26130	52261	52261	52261	52261	26130	52261	26130	26130	
IL-31	9814	9814	9814	9814	9814	3790	9814	9814	4907	9814	9814	9814	9814	4907	9814	4907	9814	9814	4907	9814	9814	
IL-33	22250	22250	22250	44500	44500	5563	22250	22250	52890	22250	59654	52890	22250	44500	44500	59654	44500	22250	52890	44500	22250	
IL-33R	6724.68	411.98	411.98	6724.68	411.98	133.69	411.98	411.98	411.98	411.98	411.98	411.98	411.98	12619.57	411.98	411.98	411.98	12619.57	411.98	411.98	12619.57	
M-CSF	29.39	15	29.39	15	15	11	15	15	29.39	29.39	29.39	15	15	156.43	29.39	15	15	29.39	15	156.43	15	
RANKL	38.5	145.42	20	20	145.42	3	20	20	145.42	20	20	20	20	145.42	38.5	20	145.42	4.72	20	20	20	
TNF alpha	335.96	168	168	168	335.96	193.59	335.96	168	335.96	168	168	168	335.96	168	168	168	168	335.96	168	168	168	
CCL11	2609	2850	629	629	629	1285	629	629	629	629	629	629	2850	2850	2850	3145	3145	629	629	3145	2850	
CXCL1	121	241.58	241.58	121	241.58	21.61	121	53.13	121	241.58	121	241.58	121	649.12	241.58	121	121	241.58	121	121	121	
CXCL10	194	194	194	194	194	108	194	1030.44	1030.44	194	386.82	194	194	1030.44	1030.44	194	194	1030.44	194	194	194	
CCL2	257.1	257.1	129.0	257.1	257.1	523.0	257.1	257.1	257.1	257.1	257.1	257.1	257.1	257.1	257.1	257.1	257.1	257.1	257.1	129.0	1736.5	
CCL7	253.5	253.5	253.5	127.0	253.5	253.5	127.0	127.0	253.5	253.5	253.5	253.5	253.5	253.5	253.5	253.5	253.5	127.0	127.0	253.5	253.5	
CCL4	115.6	115.6	1.05	1.05	1.05	8.21	115.6	1.05	178.69	1.05	1.05	1.05	1.05	1.05	1.05	1.05	1.05	54.97	115.6	1.05	1.05	
CXCL2	64.19	33	33	33	64.19	10	64.19	33	33	33	33	33	33	64.19	33	33	33	33	33	64.19	33	
Leptin	54.0	54.0	54.0	54.0	54.0	1508.0	54.0	107.6	3139.4	54.0	107.6	54.0	54.0	3139.4	107.6	107.6	54.0	3139.4	54.0	54.0	54.0	
VEGF-A	1709.1	1709.1	855.0	1709.1	855.0	5.0	1709.1	1709.1	1709.1	1709.1	1709.1	1709.1	1709.1	855.0	855.0	855.0	1709.1	1709.1	1709.1	855.0	1709.1	

Continued Supplemental Table 2

dpi	Mock																		
Sex	Male									Female									
ID	44	45	46	47	48	49	50	51	52	53	54	55	56	57	58	59	60	61	
BAFF	615.6	497.42	249	497.42	135.94	68	135.94	135.94	135.94	249	249	249	249	135.94	68	135.94	135.94	135.94	
G-CSF	10	18.65	10	18.65	49	97.67	49	97.67	49	10	18.65	10	10	49	97.67	97.67	97.67	49	
GM-CSF	4.58	331.21	4.58	4.58	310	310	310	310	310	4.58	331.21	331.21	4.58	310	310	310	310	310	
IFN-alpha	509	509	509	509	74	1047.5	1661.8	1661.8	146.13	1017.3	1017.3	509	509	146.13	146.13	1661.8	146.13	146.13	
IFN-gamma	11.44	67.2	11.44	11.44	67.85	34	34	34	67.85	11.44	6	38.39	38.39	67.85	34	34	34	67.85	
IL-1 alpha	721.98	1411.8	102	102	319	319	319	319	638.47	721.98	102	102	721.98	638.47	319	319	319	319	
IL-1 beta	27	53.94	27	27	40	40	40	40	78.3	40	40	53.94	53.94	40	78.3	40	40	40	
IL-2R	62.66	101.63	32	62.66	124.02	63	63	63	124.02	31.71	32	32	62.66	124.02	124.02	63	124.02	63	
IL-5	237	473.2	237	237	283	283	565.84	283	283	237	295.31	237	237	283	283	283	283	283	
IL-6	556	1110.4	556	556	284.3	284.3	284.3	284.3	284.3	556	556	556	556	284.3	284.3	284.3	284.3	284.3	
IL-7	246.5	246.5	246.5	124.0	581.0	581.0	581.0	581.0	581.0	246.5	246.5	246.5	246.5	581.0	581.0	581.0	581.0	581.0	
IL-9	127.4	127.4	366.9	127.4	286.4	286.4	286.4	286.4	286.4	127.4	127.4	127.4	127.4	286.4	286.4	286.4	286.4	286.4	
IL-10	786.0	1571.2	786.0	786.0	528.1	528.1	528.1	528.1	528.1	786.0	786.0	786.0	786.0	528.1	528.1	265.0	528.1	528.1	
IL-12p70	23	45.09	23	23	13	13	13	13	13	23	23	23	23	25.88	13	13	13	13	
IL-15/IL-15R	252.85	815.39	252.85	252.85	148.12	148.12	148.12	148.12	148.12	252.85	252.85	252.85	252.85	148.12	148.12	148.12	148.12	75	
IL-17A	147	293.8	147	147	137	137	137	137	137	147	147	147	147	137	137	272.33	272.33	137	
IL-18	279	279	279	279	279	279	279	4751	279	279	279	279	279	279	279	279	279	279	
IL-19	4132	4132	4132	8263	3286	3286	15274	3286	3286	8263	4132	4132	8263	3286	3286	6571	3286	3286	
IL-23	644	2672	644	644	226	113	113	226	113	644	644	644	644	113	226	226	226	113	
IL-25	413	413	207	207	12	6	12	12	12	207	207	207	207	12	12	501	12	12	
IL-28	5787	11573	5787	5787	2966	2966	2966	2966	2966	5787	5787	5787	5787	2966	2966	2966	2966	2966	
IL-31	3790	7579	3790	3790	3790	3790	3790	3790	3790	3790	3790	3790	3790	3790	3790	3790	3790	3790	
IL-33	11125	12195	5563	5563	9867	9867	9867	9867	5563	5563	5563	5563	5563	5563	5563	5563	9867	5563	
IL-33R	133.69	2662.79	67	133.69	4435	2218	4435	2218	4435	134	134	134	134	2218	2218	2218	2218	4435	
M-CSF	11	21.22	11	11	29.6	15	15	15	15	11	11	11	21.22	15	15	15	15	15	
RANKL	3	12.03	3	12.03	24	24	24	24	24	3	3	3	3	24	24	24	24	24	
TNF alpha	97	709.7	97	97	172.66	172.66	172.66	172.66	87	97	97	193.59	193.59	172.66	87	172.66	87	87	
CCL11	938	1285	713	2850	1015	713	1015	158	713	713	820	1285	938	713	158	158	1015	713	
CXCL1	143.89	292.89	143.89	72	103	103	103	109.37	103	72	72	72	143.89	103	204.87	103	103	103	
CXCL10	108	215.15	108	108	96	96	96	65.95	65.95	108	108	108	215.15	96	96	96	96	96	
CCL2	523.0	1045.1	523.0	523.0	990.0	990.0	990.0	990.0	1045.1	523.0	508.6	523.0	990.0	990.0	990.0	990.0	990.0	990.0	
CCL7	253.5	821.4	253.5	1154.5	253.5	253.5	253.5	253.5	253.5	253.5	253.5	253.5	253.5	253.5	253.5	253.5	253.5	253.5	
CCL4	37.49	37.49	8.21	8.21	35	35	35	35	35	8.21	23.66	8.21	8.21	69.45	35	35	69.45	35	
CXCL2	10	70.86	18.29	10	20	20	20	38.95	38.95	10	10	18.29	10	38.95	38.95	38.95	20	20	
Leptin	1508.0	3015.3	1508.0	1508.0	2456.0	2456.0	2456.0	2456.0	2456.0	1508.0	1508.0	1508.0	1508.0	2456.0	2456.0	2456.0	2456.0	2456.0	
VEGF-A	390.3	1361.4	196.0	390.3	390.3	196.0	390.3	390.3	196.0	390.3	196.0	390.3	390.3	390.3	390.3	390.3	390.3	390.3	

**Supplemental Table 3.** Raw cytokine concentrations in lungs.

dpi	3												7											
Sex	Male												Male											
ID	1	2	3	4	5	6	7	8	9	10	11	12	24	25	26	27	28	29	30	31	32	33		
BAFF	352	174.2	31.85	31.85	174.2	174.2	31.85	249	715.55	615.6	715.55	497.42	352	174.2	352	31.85	31.85	174.2	174.2	174.2	174.2	174.2		
G-CSF	48	95.67	95.67	48	48	95.67	95.67	18.65	18.65	18.65	10	10	48	95.67	95.67	95.67	48	95.67	95.67	95.67	95.67	48		
GM-CSF	183.55	94	183.55	183.55	183.55	183.55	183.55	331.21	4.58	4.58	4.58	4.58	183.55	183.55	183.55	576.12	183.55	183.55	183.55	183.55	183.55	183.55		
IFN-α	144.0	144.0	1027.6	287.4	287.4	287.4	1027.6	33.0	33.0	1017.3	33.0	1017.3	1027.6	287.4	144.0	1027.6	1027.6	287.4	1027.6	287.4	1027.6	695.1		
IFN-γ	92	265	456	46	265	46	46	38	20	38	20	38	4141	4755	15211	27634	11054	3583	15211	9896	18654	9896		
IL-1α	288	288	676.58	676.58	288	288	288	288	288	288	721.98	721.98	676.58	288	676.58	825	825	288	575.08	575.08	676.58	575.08		
IL-1β	42.34	42.34	42.34	42.34	42.34	42.34	42.34	53.94	53.94	53.94	53.94	53.94	42.34	109.84	187.96	42.34	42.34	42.34	42.34	42.34	42.34	42.34		
IL-2	94	94	187.52	187.52	187.52	94	94	174.77	174.77	103.36	41.18	174.77	94	94	187.52	187.52	94	187.52	94	187.52	91.93	187.52		
IL-3	20.52	20.52	20.52	20.52	20.52	20.52	20.52	24.15	24.15	88.01	24.15	24.15	278.77	20.52	20.52	20.52	278.77	278.77	278.77	278.77	20.52	336.62		
IL-4	264.36	264.36	264.36	264.36	133	133	133	43	43	43	159.66	43	133	264.36	133	264.36	264.36	133	264.36	56.51	264.36	264.36		
IL-5	476.72	22	704.65	22	43.28	43.28	43.28	295.31	237	237	237	728.11	22	43.28	476.72	476.72	476.72	43.28	476.72	476.72	476.72	476.72		
IL-6	1529.6	2548.3	4270.7	112.1	2548.3	2548.3	112.1	556.0	1110.4	556.0	1110.4	2383.0	2548.3	2548.3	112.1	4270.7	3445.2	112.1	2548.3	112.1	4270.7	4270.7		
IL-7	1185.5	1185.5	1185.5	1185.5	1185.5	1185.5	1185.5	246.5	124.0	246.5	246.5	124.0	1185.5	1185.5	1185.5	2682.0	593.0	1185.5	593.0	1185.5	1185.5	1185.5		
IL-7Rα	2597	751	751	751	751	751	751	342	342	342	342	342	751	2597	751	2597	751	751	751	2597	2597			
IL-10	531	531	531	531	531	531	531	531	531	531	531	531	531	531	531	266	531	531	531	531	531	2394		
IL-12p70	30.22	30.22	30.22	30.22	16	16	16	23	23	23	23	23	30.22	30.22	136.7	30.22	30.22	30.22	30.22	30.22	16	30.22		
IL-13	30.7	30.7	30.7	30.7	30.7	131.31	30.7	21.46	21.46	21.46	21.46	21.46	30.7	30.7	30.7	16	30.7	30.7	30.7	131.31	30.7	30.7		
IL-15	101	200.69	200.69	200.69	200.69	200.69	200.69	252.85	252.85	252.85	252.85	127	512.64	200.69	200.69	512.64	512.64	200.69	512.64	200.69	704.54	512.64		
IL-17A	575.0	1149.7	575.0	1149.7	575.0	575.0	1149.7	147.0	293.8	147.0	147.0	293.8	1149.7	1149.7	575.0	575.0	575.0	1149.7	575.0	1149.7	1149.7	1149.7		
IL-18	153.0	305.9	305.9	305.9	305.9	305.9	305.9	130.0	130.0	130.0	130.0	130.0	153.0	153.0	305.9	153.0	305.9	305.9	1374.9	305.9	305.9	305.9		
IL-22	377	377	377	377	377	189	377	263	263	263	263	227	377	377	1013	697	377	377	377	377	1678	377		
IL-23	595.5	595.5	595.5	298.0	595.5	595.5	595.5	323.0	644.2	644.2	644.2	644.2	595.5	595.5	595.5	7647.0	6627.6	595.5	595.5	595.5	595.5	595.5		
IL-25	405.89	101	405.89	405.89	101	200.34	405.89	207	207	207	207	207	200.34	405.89	405.89	101	101	101	405.89	200.34	101	405.89		
IL-27	30.58	110.35	56	56	56	247.82	56	67	67	67	36.6	369.93	56	56	56	56	110.35	247.82	110.35	448.1	110.35	56		
IL-28	68	4575	11130	68	68	4575	5787	5787	13506	11573	11573	21752	4575	11130	68	4575	68	68	1202	68	4575	4575		
IL-33	11681	11681	24685	17810	11681	24685	11681	5563	13114	11125	5563	12195	43999	24685	24685	24685	24685	24685	24685	24685	11681	43999		
IL-33R	278.8	6125.4	278.8	278.8	278.8	278.8	278.8	133.7	3690.0	2662.8	133.7	133.7	278.8	278.8	278.8	278.8	278.8	278.8	278.8	278.8	278.8	278.8		
LIF	131.37	11.13	11.13	11.13	11.13	131.37	131.37	21.94	105.66	21.94	105.66	21.94	11.13	66.56	6	131.37	293.58	6	131.37	293.58	131.37	66.56		
M-CSF	13.39	1.95	1.95	1.95	1.95	13.39	13.39	11	11	21.22	21.22	11	13.39	1.95	6.61	1	13.39	6.61	13.39	1	6.61	1.95		
RANKL	28.56	28.56	28.56	10.78	28.56	28.56	28.56	12.03	142.6	32.85	87.69	32.85	28.56	54.7	28.56	89.28	54.7	28.56	89.28	28.56	28.56	54.7		
TNFα	197.37	197.37	197.37	197.37	99	197.37	197.37	193.59	193.59	97	193.59	193.59	197.37	197.37	197.37	197.37	400.69	99	197.37	197.37	400.69	197.37		
CXCL5	250.0	1300.7	1300.7	250.0	498.3	1300.7	1300.7	75.0	762.6	762.6	75.0	762.6	1300.7	250.0	1300.7	2274.9	1300.7	250.0	1300.7	1300.7	1300.7	1300.7		
CCL11	4275	2850	4275	2850	2850	4275	4275	4275	4275	4275	4275	4275	2850	2850	2850	4275	4275	4275	4275	2850	4275	2850		
CXCL1	1347.3	356.0	573.9	126.3	800.4	126.3	126.3	292.9	1297.2	501.0	292.9	362.3	356.0	356.0	356.0	64.0	356.0	356.0	356.0	244.7	356.0	356.0		
CCL2	536	268	1496	268	536	268	268	523	523	523	523	2674	536	1496	1496	3044	2517	268	2517	1496	4666	2517		
CCL7	1208.0	501.0	972.2	30.8	736.5	30.8	30.8	1154.5	2931.9	2034.3	3120.7	3300.1	736.5	501.0	972.2	972.2	736.5	854.4	972.2	972.2	972.2	972.2		
CCL3	85.23	53.28	85.23	23.68	23.68	38.52	15.56	5.13	28.56	20.11	118.78	260.92	122.68	168.13	317.76	144.23	133.19	68.72	296.64	168.13	296.64	168.13		
CCL4	100.68	67.19	67.19	34	100.68	67.19	34	8.21	37.49	8.21	37.49	120.63	124.83	124.83	156.46	187.11	166.63	100.68	230.88	187.11	208.32	208.32		
CXCL2	43.24	22	43.24	22	43.24	22	43.24	18.29	18.29	18.29	10	18.29	43.24	43.24	43.24	43.24	43.24	22	43.24	22	43.24	43.24		
CCL5	441.2	265.2	286.6	340.8	407.4	308.1	286.6	314.4	615.0	412.5	1342.1	1010.5	202.3	340.8	385.0	141.8	233.5	319.0	396.2	244.0	297.3	223.1		
BTC	118.67	118.67	118.67	60	118.67	118.67	60	117.44	117.44	117.44	117.44	243.21	60	60	118.67	118.67	118.67	60	118.67	118.67	118.67	118.67		
VEGF-A	427.91	427.91	427.91	427.91	427.91	588.15	427.91	287.85	287.85	287.85	513.4	513.4	427.91	427.91	427.91	427.91	427.91	588.15	427.91	427.91	588.15	427.91		

Continued Supplemental Table 3

dpi	3												7											
Sex	Female												Female											
ID	13	14	15	16	17	18	19	20	21	22	23	34	35	36	37	38	39	40	41	42	43			
BAFF	31.85	16	31.85	31.85	31.85	352	4791.49	2462.5	497.42	497.42	344.29	174.2	31.85	31.85	31.85	31.85	31.85	31.85	31.85	174.2	31.85			
G-CSF	95.67	95.67	48	48	48	95.67	92.41	47	18.65	18.65	18.65	95.67	95.67	95.67	48	95.67	95.67	95.67	48	95.67	48			
GM-CSF	183.55	183.55	183.55	183.55	183.55	183.55	135	927.18	4.58	158.1	4.58	183.55	183.55	183.55	183.55	183.55	183.55	183.55	183.55	183.55	183.55			
IFN-alpha	1027.6	1027.6	1027.6	287.4	695.1	695.1	920.0	1838.6	1017.3	33.0	33.0	144.0	1027.6	287.4	144.0	287.4	144.0	287.4	287.4	144.0	1027.6			
IFN-gamma	265	46	265	265	46	46	104	104	20	20	38	1183	2616	670	2616	265	4755	6168	1183	1825	1183			
IL-1 alpha	288	288	288	288	676.58	825	1677.15	1677.15	721.98	288	721.98	676.58	676.58	288	676.58	288	288	288	288	676.58	288			
IL-1 beta	42.34	42.34	42.34	42.34	42.34	42.34	224.7	224.7	237.3	53.94	53.94	42.34	42.34	42.34	42.34	42.34	42.34	187.96	42.34	42.34	42.34			
IL-2	94	94	187.52	94	187.52	94	225.41	113	174.77	174.77	41.18	187.52	187.52	94	94	187.52	187.52	187.52	187.52	187.52	94			
IL-3	20.52	278.77	20.52	20.52	278.77	20.52	2.43	2.43	88.01	24.15	24.15	20.52	20.52	278.77	20.52	20.52	20.52	20.52	20.52	20.52	20.52			
IL-4	264.36	133	133	264.36	56.51	264.36	1089.99	54	43	159.66	43	264.36	133	264.36	133	56.51	264.36	264.36	264.36	133	133			
IL-5	22	43.28	476.72	22	43.28	43.28	800.98	44.56	237	237	237	476.72	43.28	43.28	43.28	254.47	476.72	43.28	43.28	476.72	22			
IL-6	2548.3	2548.3	2548.3	112.1	112.1	112.1	4278.6	4278.6	1110.4	556.0	556.0	1529.6	112.1	112.1	2548.3	1529.6	2548.3	112.1	112.1	57.0	112.1			
IL-7	1185.5	1185.5	1185.5	1185.5	1185.5	1185.5	254.7	254.7	2313.1	246.5	124.0	1185.5	1185.5	1185.5	593.0	1185.5	1185.5	1185.5	1185.5	1185.5	1185.5			
IL-7R alpha	751	751	751	751	751	751	3325	3325	342	342	342	751	751	2597	751	751	2597	751	751	751	751			
IL-10	531	531	266	531	531	531	1077	2152	531	531	531	266	531	531	531	531	531	531	531	531	531			
IL-12p70	30.22	16	30.22	136.7	16	30.22	102.41	60	23	23	23	16	30.22	30.22	30.22	30.22	30.22	30.22	30.22	30.22	30.22			
IL-13	16	30.7	30.7	30.7	30.7	16	124	124	21.46	21.46	21.46	30.7	16	30.7	30.7	30.7	30.7	30.7	30.7	131.31	30.7			
IL-15/IL-15R	200.69	200.69	200.69	200.69	200.69	200.69	148.4	148.4	252.85	252.85	252.85	200.69	200.69	200.69	200.69	200.69	704.54	200.69	200.69	200.69	200.69			
IL-17A	575.0	575.0	575.0	575.0	575.0	1149.7	478.5	478.5	147.0	147.0	575.0	1149.7	575.0	575.0	575.0	575.0	1149.7	575.0	575.0	575.0	575.0			
IL-18	305.9	153.0	153.0	305.9	153.0	305.9	130.0	165.4	130.0	130.0	130.0	153.0	305.9	305.9	305.9	305.9	1374.9	305.9	305.9	153.0	305.9			
IL-22	377	377	377	377	377	377	207	414	525	263	263	377	377	377	377	189	377	1013	1013	377	1013			
IL-23	595.5	595.5	595.5	595.5	595.5	6627.6	1143.6	4873.8	644.2	644.2	644.2	595.5	6627.6	298.0	595.5	595.5	6627.6	6627.6	595.5	595.5	298.0			
IL-25	405.89	101	566.98	101	200.34	101	359.31	359.31	207	412.75	207	101	101	405.89	405.89	101	101	405.89	101	200.34	101			
IL-27	56	56	56	56	56	56	698.23	134.8	133.11	67	133.11	56	247.82	110.35	56	56	56	56	56	110.35	56			
IL-28	68	68	35	68	68	68	89993	54025	11573	11573	5787	68	68	68	68	68	68	68	68	4575	68			
IL-33	11681	11681	11681	24685	24685	11681	5563	9755	11125	11125	5563	11681	24685	24685	17810	24685	24685	17810	24685	11681	11681			
IL-33R	278.8	278.8	278.8	278.8	278.8	278.8	3063.0	3063.0	1732.4	133.7	133.7	278.8	278.8	6125.4	278.8	278.8	278.8	278.8	278.8	278.8	278.8			
LIF	11.13	131.37	6	131.37	6	66.56	52	102.66	105.66	21.94	21.94	131.37	131.37	131.37	6	131.37	11.13	131.37	131.37	131.37	66.56			
M-CSF	1.95	6.61	1	1	1	13.39	91.48	46	11	11	11	1.95	1.95	1	1	1.95	1.95	1.95	1	1.95	13.39			
RANKL	28.56	28.56	10.78	10.78	10.78	10.78	17	17	78.34	118.95	21.52	1.98	10.78	10.78	28.56	28.56	28.56	54.7	28.56	28.56	54.7			
TNF alpha	197.37	197.37	197.37	197.37	197.37	197.37	166.73	166.73	193.59	193.59	193.59	197.37	197.37	99	197.37	197.37	197.37	197.37	99	99	197.37			
CXCL5	250.0	1300.7	250.0	250.0	1300.7	250.0	2755.8	2755.8	75.0	75.0	762.6	498.3	1300.7	1300.7	250.0	1300.7	1300.7	1300.7	1300.7	1300.7	1300.7			
CCL11	4275	2850	858	2850	2850	2850	4275	4275	2850	4275	4275	2850	2850	2850	2850	713	2850	2850	2850	2850	2850			
CXCL1	126.3	64.0	126.3	126.3	356.0	64.0	142.7	142.7	21.6	143.9	143.9	126.3	126.3	126.3	356.0	64.0	126.3	356.0	126.3	126.3	356.0			
CCL2	268	268	268	268	268	268	288	574	1045	523	523	268	268	104	268	268	1496	104	268	268	536			
CCL7	30.8	30.8	30.8	30.8	501.0	30.8	825.0	1048.6	1154.5	821.4	821.4	30.8	501.0	501.0	265.7	501.0	501.0	736.5	501.0	501.0	736.5			
CCL3	4.43	4.43	4.43	4.43	23.68	4.43	27.08	93.75	37.45	37.45	5.13	23.68	38.52	68.72	38.52	38.52	133.19	168.13	103.12	53.28	85.23			
CCL4	34	34	34	34	34	34	8	14.91	8.21	8.21	37.49	34	34	34	34	67.19	146.19	187.11	67.19	100.68	100.68			
CXCL2	22	22	43.24	43.24	22	22	206.92	206.92	18.29	18.29	10	22	43.24	22	22	43.24	43.24	43.24	43.24	43.24	22			
CCL5	407.4	407.4	286.6	141.8	362.9	286.6	436.2	414.7	970.5	655.7	957.4	244.0	181.9	202.3	254.6	265.2	265.2	319.0	351.8	373.9	396.2			
Betacellulin	118.67	118.67	60	118.67	118.67	60	140.65	71	185.23	117.44	59	197.31	118.67	118.67	60	118.67	197.31	118.67	118.67	60	118.67			
VEGF-A	427.91	427.91	588.15	427.91	427.91	588.15	1520.14	6349.8	513.4	813.75	287.85	427.91	588.15	427.91	427.91	427.91	588.15	427.91	427.91	427.91	588.15			

Continued Supplemental Table 3

dpi	Mock																	
Sex	Male									Female								
ID	44	45	46	47	48	49	50	51	52	53	54	55	56	57	58	59	60	61
BAFF	249	497.42	249	715.55	135.94	135.94	135.94	748.28	68	249	497.42	249	497.42	135.94	68	135.94	135.94	135.94
G-CSF	10	10	18.65	108.99	49	97.67	97.67	97.67	97.67	10	18.65	10	18.65	49	97.67	97.67	49	49
GM-CSF	3	4.58	4.58	513.51	310	310	310	310	310	4.58	3	4.58	4.58	310	310	310	310	310
IFN-alpha	33.0	33.0	1017.3	1956.5	146.1	146.1	1661.8	74.0	74.0	33.0	1017.3	1017.3	33.0	74.0	74.0	146.1	74.0	1661.8
IFN-gamma	20	25	20	67	34	34	34	34	34	20	20	20	20	34	34	34	34	34
IL-1 alpha	721.98	288	288	1411.8	288	288	288	288	288	288	288	288	288	288	288	288	288	288
IL-1 beta	27	27	27	237.3	397.87	78.3	78.3	40	40	27	27	53.94	27	40	397.87	40	40	40
IL-2	21	41.18	21	336.14	102.67	102.67	52	102.67	52	41.18	41.18	41.18	41.18	52	102.67	102.67	52	102.67
IL-3	24.15	24.15	24.15	101.04	10.62	10.62	10.62	10.62	10.62	24.15	24.15	24.15	24.15	10.62	10.62	10.62	10.62	10.62
IL-4	43	43	43	159.66	145	289.3	145	289.3	145	43	159.66	159.66	43	145	289.3	289.3	145	145
IL-5	237	237	237	728.11	283	283	283	283	283	237	237	237	237	283	283	283	283	283
IL-6	556.0	1110.4	556.0	2001.4	284.3	284.3	284.3	284.3	284.3	556.0	556.0	556.0	556.0	284.3	284.3	284.3	284.3	3186.1
IL-7	246.5	246.5	124.0	2908.4	581.0	581.0	581.0	581.0	581.0	246.5	124.0	246.5	246.5	581.0	581.0	581.0	581.0	581.0
IL-7R alpha	342	342	342	4163	365	365	365	365	365	342	342	342	342	365	365	365	365	365
IL-10	531	531	531	2360	528	528	528	528	528	531	531	531	531	528	528	528	528	528
IL-12p70	23	23	23	104.24	23	23	23	23	23	23	23	23	23	23	23	23	23	23
IL-13	21.46	21.46	21.46	209.43	2	3.01	3.01	2	3.01	21.46	11	21.46	21.46	2	2	3.01	3.01	3.01
IL-15/IL-15R	252.85	252.85	252.85	917.06	148.12	148.12	75	148.12	148.12	252.85	252.85	252.85	252.85	148.12	148.12	148.12	148.12	75
IL-17A	209.4	293.8	147.0	414.6	137.0	137.0	137.0	137.0	137.0	209.4	293.8	147.0	147.0	137.0	137.0	137.0	137.0	137.0
IL-18	130.0	130.0	130.0	130.0	279.0	279.0	279.0	279.0	279.0	130.0	130.0	130.0	130.0	279.0	279.0	279.0	279.0	279.0
IL-22	263	263	263	1076	822	822	822	822	822	263	263	263	263	822	822	822	822	822
IL-23	644.2	644.2	644.2	2962.5	226.0	226.0	226.0	226.0	226.0	644.2	644.2	2672.1	644.2	226.0	226.0	226.0	226.0	226.0
IL-25	207	207	412.75	677.91	207	207	207	207	207	207	207	412.75	207	501.4	207	207	501.4	501.4
IL-27	67	67	67	640.84	64	127.6	64	64	64	67	67	67	67	64	64	64	64	64
IL-28	5787	5787	11573	11573	2966	2966	2966	2966	2966	5787	5787	11573	5787	2966	2966	2966	2966	2966
IL-33	5563	11125	11125	13114	9867	44500	9867	9867	9867	5563	5563	5563	5563	9867	9867	9867	4934	37246
IL-33R	133.7	133.7	133.7	3690.0	2218.0	2218.0	2218.0	2218.0	2218.0	133.7	133.7	1732.4	133.7	2218.0	2218.0	1821.5	2218.0	2218.0
LIF	105.66	60.19	21.94	331.8	51	51	51	51	51	60.19	105.66	21.94	21.94	51	100.1	100.1	51	51
M-CSF	11	11	11	41.85	15	15	15	29.6	15	11	11	11	11	15	15	29.6	29.6	29.6
RANKL	46.06	46.06	32.85	97.56	24	24	24	24	24	32.85	46.06	46.06	142.6	24	24	24	24	24
TNF alpha	193.59	193.59	193.59	709.7	172.66	87	172.66	172.66	87	193.59	193.59	193.59	193.59	172.66	87	87	172.66	172.66
CXCL5	75.0	762.6	762.6	2011.8	578.8	1005.1	578.8	503.0	503.0	762.6	762.6	75.0	75.0	503.0	503.0	503.0	503.0	1005.1
CCL11	2850	2850	2850	4275	2850	2850	2850	2850	713	4275	938	4275	938	2850	1015	2850	4275	4275
CXCL1	72.0	643.8	143.9	431.4	103.0	103.0	204.9	381.4	103.0	72.0	72.0	98.0	72.0	103.0	103.0	103.0	103.0	204.9
CCL2	523	523	523	1918	990	990	990	990	990	523	523	1045	1045	990	990	990	1979	990
CCL7	253.5	253.5	821.4	1292.7	180.8	180.8	180.8	180.8	91.0	253.5	253.5	253.5	253.5	180.8	91.0	180.8	180.8	180.8
CCL3	5.13	5.13	5.13	28.56	243.4	29.45	29.45	29.45	15	20.11	20.11	5.13	20.11	29.45	15	29.45	29.45	29.45
CCL4	5	8.21	8.21	64.55	35	35	35	35	35	37.49	8.21	8.21	8.21	35	35	31.94	35	35
CXCL2	10	18.29	18.29	70.86	20	38.95	38.95	38.95	20	18.29	10	10	10	38.95	20	20	20	38.95
CCL5	267.7	354.5	191.7	191.7	465.0	160.0	513.9	416.4	128.4	267.7	412.5	429.6	412.5	651.4	343.3	465.0	538.5	588.2
Betacellulin	243.21	59	117.44	349.72	59	59	59	59	59	59	117.44	59	117.44	59	59	59	59	59
VEGF-A	287.85	287.85	61.81	813.75	1536.29	1178.15	1536.29	1361.43	1178.15	813.75	513.4	813.75	513.4	1361.43	1361.43	1536.29	1361.43	1536.29

## Curriculum Vitae

Aihui Wang  
Baltimore, MD 21202  
443-333-3693  
awang88@jh.edu

### EDUCATION

---

**Johns Hopkins University, Bloomberg School of Public Health** Sep. 2019-Present  
• Sc.M. in Biochemistry and Molecular Biology

**Shanghai Jiao Tong University, School of Medicine** Sep. 2015-Jun. 2019  
• B.S. in Medical Laboratory Tech

### ACADEMIC EXPERIENCES

---

#### Research Experiences:

**Sex Differences in the Influenza B Virus (IBV) Pathogenesis** Jun. 2020-Present  
*Johns Hopkins University, Bloomberg School of Public Health*

*Advisor: Dr. Sabra Klein, Professor*

#### Contribution:

- Established mouse model of IBV, including conducting mLD50 tests, using morbidity and mortality
- Mastery of infection protocols for both mice (in vivo) and cell culture (in vitro), with analysis of virus titration and quantification in tissues and cells and optimization of protocols specific for IBV
- Mastery of animal handling, dissection, and tissue and blood collection techniques
- Utilization of basic microbiological and immunological assays including TCID50, ELISA, microneutralization, and cytokine multiplex assays

**Correlation Analysis of Vaginal Microbiome Diversity and Cervical Intraepithelial Neoplasia** Oct. 2018-Apr. 2019  
*Obstetrics and Gynecology Hospital of Fudan University, Clinical Lab*

*Advisor: Dr. Chunmei Ying, Chair*

#### Contribution:

- Collected and stored clinical vaginal swab specimens
- Analyzed the diversity data of vaginal microbiome from 32 cases; compared alpha and beta diversity between different levels of cervical intraepithelial neoplasia

**Method Development for the Detection of a MyD88 Point Mutation using allele specific-PCR** Jun. 2017-Jul. 2017  
*Shanghai Ruijin Hospital*

*Advisor: Dr. Lei Dong, Associate Chief Physician*

#### Contribution:

- Retrieved genetic databases for the sequence of a specific Myd88 point mutation; designed TaqMan probes, quality control plasmids, and six PCR primer pairs in Amplification Refractory Mutation System (ARMS) method for the detection of Myd88 point mutation
- Performed qRT-PCR to detect diluted plasmids; verified the eligibility of each primer pair
- Determined the optimal initial concentration of ARMS primer pair



## **Microfluidic Chip Design for Early Detection of Breast Cancer in Digital PCR Method**

*Shanghai Jiao Tong University School of Biomedical Engineering*

**May 2017-Dec. 2018**

*Advisor: Dr. Xianting Ding, Professor*

### **Contribution:**

- Wrote research proposal, mainly tasked with the study design
- Compared several detection methodologies and suggested to combine microdroplet chip with digital PCR
- Improved the existing chip design and drew the sketch for chip fabrication
- Finished two literature reviews

### **Conference Presentations:**

- Woldetsadik Y, **Wang A**, Perez D, Cardenas-Garcia S, Klein SL. Characterizing sex differences in Influenza B virus pathogenesis in C57BL/6 mice. Centers of Excellence for Influenza Research and Surveillance (CEIRS) (2021) **\*Poster awarded\***
- **Wang A**, Cardenas-Garcia S, Rajao D, Perez D Klein SL. The effect of biological sex on influenza B virus pathogenesis in C57BL/6 mice. American Society for Virology (2021) **\*Poster Presentation\***

### **Peer Reviewed Publications:**

- **Wang A**, Abdulla A, Ding X. Microdroplets-on-chip: A review. Proceedings of the Institution of Mechanical Engineers, Part H: Journal of Engineering in Medicine. 2019;233(7):683-694.  
doi:10.1177/0954411919850912

### **Ad hoc peer review:**

- Journal of Virology: Defective NKp46 recognition and elimination of influenza B viruses (2020)
- EBioMedicine: Shorter androgen receptor polyQ alleles protect against life-threatening COVID-19 disease in males (2020)
- Scientific Report: Male to female ratio of influenza morbidity switches between children and adults (2020)

## **INTERSHIPS**

---

### **Roche Diagnostics, Shanghai**

**Nov. 2018-Jun. 2019**

*Assistant to Bidding Operation Team*

- Established and optimized the database of 200 products
- Assisted with the confirmation of actions for identified tenders in the first and second quarter of 2019, followed up bidding results, and conducted bidding data analysis

### **Obstetrics and Gynecology Hospital of Fudan University**

**May 2018-Nov. 2018**

*Intern in Clinical Lab*

- Outpatient Care: took charge of finger blood routine and urine routine examinations
- Blood Specimen Lab: collected and pre-processed the clinical specimens; read blood smears; used automatic instruments to perform immunological and biochemical examination, issued test reports and provided consultations for physicians; performed quality control and maintenance for instruments
- Microbe Lab: took charge of specimen inoculation and chlamydia examination

### **Shanghai Ruijin Hospital**

**Jul. 2017-Aug. 2017**

*Intern in Clinical Lab*

- Responsible for specimen collection and pretreatment, finger blood collection
- Used automatic instruments to perform biochemical examination, nearly 1000 specimens daily

## SKILLS

---

### **Experimental Skills**

- Blood smear staining and morphology examination
- Bacteria and cell cultivation; virus propagation and titration
- Animal modeling and surgery
- Neutralizing assay, ELISA

### **Software**

- Stata 15, R, Primer 5, Prism, Microsoft Office